

A *uvbyCaH β* CCD Analysis of the Open Cluster Standard, NGC 752 ¹

Bruce A. Twarog

Department of Physics and Astronomy, University of Kansas, Lawrence, KS 66045-7582, USA

btwarog@ku.edu

Barbara J. Anthony-Twarog

Department of Physics and Astronomy, University of Kansas, Lawrence, KS 66045-7582, USA

bjat@ku.edu

Constantine P. Deliyannis

Department of Astronomy, Indiana University, Bloomington, IN 47405-7105

cdeliyan@indiana.edu

and

David T. Thomas

Department of Physics and Astronomy, University of Kansas, Lawrence, KS 66045-7582, USA

wendysdbcb@outlook.com

ABSTRACT

Precision *uvbyCaH β* photometry of the nearby old open cluster, NGC 752, is presented. The mosaic of CCD fields covers an area $\sim 42'$ on a side with internal precision at the 0.005 to 0.010 mag level for the majority of stars down to $V \sim 15$. The CCD photometry is tied to the standard system using an extensive set of published photoelectric observations adopted as secondary standards within the cluster. Multicolor indices are used to eliminate as nonmembers a large fraction of the low probability proper-motion members near the faint end of the main sequence, while identifying 24 potential dwarf members between $V = 15.0$ and 16.5, eight of which have been noted before from Vilnius photometry. From 68 highly probable F dwarf members, we derive a reddening estimate of $E(b - y) = 0.025 \pm 0.003$ ($E(B - V) = 0.034 \pm 0.004$), where the error includes the internal photometric uncertainty and the systematic error arising from the choice of the standard ($b - y$, $H\beta$) relation. With reddening fixed, $[\text{Fe}/\text{H}]$ is derived from the F dwarf members using both m_1 and hk , leading to $[\text{Fe}/\text{H}] = -0.071 \pm 0.014$ (sem) and -0.017 ± 0.008 (sem), respectively. Taking the internal precision and possible systematics in the standard relations into account, $[\text{Fe}/\text{H}]$ for NGC 752 becomes -0.03 ± 0.02 . With

the reddening and metallicity defined, we use the Victoria-Regina isochrones on the Strömrgren system and find an excellent match for $(m - M) = 8.30 \pm 0.05$ and an age of 1.45 ± 0.05 Gyr at the appropriate metallicity.

Subject headings: open clusters: general — open clusters: individual (NGC 752)

1. Introduction

Nearby star clusters are invaluable because they permit observational access to stars of lower luminosity with a specific age and composition using the full array of photometric and spectroscopic tools, often without the need for telescopes of large aperture. With the exception of the sparsely populated open cluster, Rup 147 (Curtis et al. 2013) at $(m - M) = 7.35$, NGC 752 remains the nearest open cluster ($(m - M) = 8.4$) older than 1 Gyr, with a well-determined age of 1.45 Gyr (Anthony-Twarog et al. 2009). While it is likely that the uncertainties in the fundamental cluster properties of Rup 147 will diminish as its membership is expanded and its individual stars are studied on a variety of photometric systems, the areal spread of over 5 square degrees and the low density contrast have led to slow progress in the investigation of this intriguing object. By comparison, NGC 752 has a long history of photoelectric observations on virtually every major photometric system from broad-band UBVRI (Johnson 1953; Eggen 1963; Taylor, Joner, & Jeffery 2008) and Washington photometry (Canterna et al. 1986) to intermediate-band photometry on the extended Strömrgren (Crawford & Barnes 1970; Twarog 1983; Joner & Taylor 1995; Anthony-Twarog & Twarog 2006), Vilnius/Stromvil (Dzėrvitis & Paupers 1993; Bartašūiė et al. 2007; Zdanavičius, Bartašūiė, & Zdanavičius 2010; Bartašūiė et al. 2011), DDO (Janes 1979), and Geneva (Rufener 1981, 1988) systems. High and moderate-dispersion spectroscopy (Friel & Janes 1993; Friel et al. 2002; Sestito, Randich, & Pallavicini 2004; Carrera & Pancino 2011; Reddy, Giridhar, & Lambert 2012; Nault & Pilachowski 2013; Maderak et al. 2013; Böcek Topcu et al. 2015) is available for limited samples of both dwarfs and giants. The definitive proper-motion survey is Platais (1991) (hereinafter PL) and radial-velocity surveys include Daniel et al. (1994); Mermilliod et al. (1998, 2008, 2009), but additional radial-velocity measures for 45 stars in the field of NGC 752 are also available in Maderak et al. (2013).

Because of the magnitude and color range of the cluster color-magnitude diagram (CMD), NGC 752 should be an ideal candidate for standardization of any photometric system observed with a large format CCD on moderate to large aperture telescopes. In particular, because of its extensive list of photoelectrically studied stars on the Strömrgren system (Crawford & Barnes 1970; Twarog 1983; Joner & Taylor 1995) and, to a lesser extent, the *Caby* system (Anthony-Twarog & Twarog 2006), NGC 752 has been regularly included in the standardization of our cluster work, most recently within our program to map Li evolution over a range of age and metallicity (Anthony-Twarog et al.

¹WIYN Open Cluster Study LXIX

2009, 2010, 2013, 2014; Cummings et al. 2012; Lee-Brown et al. 2015) using open clusters with unusually well-defined fundamental parameters, critical for deriving precise, high-dispersion spectroscopic abundances.

However, despite the wealth of published data for NGC 752, as with Rup 147, its significant size of over a square degree has limited the completeness of the CCD data available on any photometric system. To date, the only significant CCD surveys within NGC 752 are the Vilnius studies of Zdanavičius, Bartašūite, & Zdanavičius (2010) and Bartašūite et al. (2011). The older study covers 1.5 square degrees with a CCD camera of low spatial resolution (3.4'' per pixel), while the more recent analysis covers four overlapping fields of 12' × 12' each in the cluster core, observed with the Vatican Advanced Technology Telescope with a CCD resolution of 0.37'' per pixel. The purpose of this paper is to present precision CCD photometry of NGC 752 on the extended Strömgren system covering a field approximately 42' × 42' on the sky to below the current magnitude limit for complete proper-motion membership data. While the survey still covers only one-third of the potential area of the cluster, it does contain approximately two-thirds of the known members brighter than $V = 15.2$, a magnitude range which may represent the actual faint limit for the main sequence members of this evaporating cluster (Francic 1989). More specifically, the expanded standards will be adopted as primary contributors to the calibration of CCD data in two key clusters, NGC 7789 and NGC 2158, within our current cluster Li investigation.

The outline of the paper is as follows: Sec. 2 discusses the CCD observations and their reduction to the standard system for intermediate-band photometry; Sec. 3 uses the photometry, in conjunction with proper-motion membership, to identify and isolate probable cluster members which become the core data set for selecting single, main sequence stars for reddening, metallicity, age, and distance estimates in Sec. 4. The extrapolated main sequence is also used to identify potential lower main sequence members of the cluster. Sec. 5 contains a summary of our conclusions.

2. Observations and Data Reduction

2.1. Observations

Intermediate and narrow-band images of NGC 752 were obtained using the WIYN 0.9-m telescope during three observing runs in Nov. 2010, Nov. 2012 and Dec. 2013. The cluster was observed as a primary source of standards for the extended Strömgren and $H\beta$ systems, along with a range of field stars from the standard catalogs for both systems. Because of the apparent brightness of the cluster stars and the wide range in color, NGC 752 was observed on all usable nights - for zero-point and color calibration on photometric nights and for color-slope estimation on non-photometric nights. For the first two observing runs, the S2KB CCD was used at the $f/7.5$ focus of the telescope for a 20' × 20' field with 0.6'' pixels. All seven filters were from the 3'' × 3'' filter set owned jointly by the University of Kansas and Mt. Laguna Observatory. For the Dec. 2013 run, the telescope was equipped with the Half-Degree-Imager (HDI), a 4K × 4K chip with a

$29' \times 29'$ field with $0.43''$ pixels. The seven filters were from the extended Strömgren set recently acquired for specific use with the HDI.

Bias frames and dome flats for each filter were obtained every night, with sky flats observed at twilight for the u , v , and Ca filters when feasible for the S2KB runs; for the Dec. 2013 run, sky flats were obtained every night for every filter in use each evening. Extinction stars and field star standards were observed every photometric night for use with clusters without internal standards and as a check on the calibrations of cooler dwarfs within NGC 752 since the photoelectric data within the cluster are dominated by red giants and F dwarfs. As discussed earlier, while the cluster is an ideal calibration source for telescopes of small to modest aperture, its small distance modulus ($(m - M) \sim 8.3$) means that the areal coverage of the cluster field is large, making it a challenge to observe more than a handful of the internal secondary photoelectric standards in a single frame. To optimize coverage, NGC 752 was initially divided into four overlapping quadrants producing a composite field just over $33'$ on a side. For the Dec. 2013 run, the same quadrant centers were adopted, expanding the degree of overlap among the quadrants and expanding the areal coverage to $\sim 42'$ on a side. It should be emphasized that while the overlap among the frames can lead to dozens of measurements in each filter for stars near the cluster core, the exposure times for the frames were designed primarily with the internal photoelectric standards in mind, i.e. stars in the $V = 8$ to 12 range, so that precision photometry to $V = 16$ is only feasible due to the large number of short exposures coupled to a limited set of longer frames designed to reach $V = 15$ and below. This contrasts with our usual approach to cluster observations where emphasis is placed on minimizing photometric scatter for stars fainter than $V \sim 16.5$.

Standard IRAF routines were used to perform initial processing of the frames, i.e. bias-subtraction and flat-fielding. Illumination corrections were applied to frames obtained in 2012, but tests with the 2013 frames showed no statistically significant difference between the photometry with or without correction, so none was applied. A fairly comprehensive discussion of our procedure for obtaining PSF-based instrumental magnitudes and merging multiple frames of a given filter can be found in Anthony-Twarog & Twarog (2000). Instrumental magnitudes and indices were constructed separately for the 2010/2012 data and for the 2013 data. The photometric indices from the S2KB chip and filters were transformed to the instrumental system defined by the HDI chip and its newer filters. The choice of fiducial instrumental system is arbitrary given the ultimate need to transfer the instrumental indices to the standard system, but the larger field size, newer filters, and greater overlap among mosaicked images made the HDI data the logical choice for defining the instrumental system. Prior to the predictable application of color-dependent corrections in transforming from one instrumental system (chip and filter set) to another, a comprehensive check was made for potential position-dependent offsets between the two data sets, a not improbable option given the nature of the overlapping CCD frames. No statistically significant discontinuities were discovered in magnitude or color at the overlap boundaries, lending credence to the validity of the frame-to-frame merger process. Position-dependent gradients across the composite S2KB field at the level of 0.05 mag were identified in the y filter, the Strömgren equivalent for V , and

eliminated using a quadratic in the X and Y positions; for color indices, trends with position were dramatically reduced or eliminated, but derived adjustments were applied whenever the residual patterns were found to be statistically significant.

Once transformed to a common instrumental system, the y magnitudes and color indices from the two data sets were combined using a weighting scheme tied to the inverse square of the derived standard errors of the mean for the individual stars in both magnitude and color.

2.2. Internal Cluster Standards - Warmer Dwarfs and Red Giants

Our standard procedure for calibrating CCD Strömrgren photometry includes adoption of a single calibration equation for all colors and luminosity classes for V , $H\beta$, and hk , with the addition of a color term for V . By contrast, for m_1 , and c_1 , separate equations with color terms are derived for warmer dwarfs ($b - y < 0.45$), for cooler ($b - y \geq 0.45$) dwarfs, and for cooler evolved stars; for $b - y$, a distinct calibration equation is sought and utilized for cooler dwarfs. The rich catalog of photoelectric observations within the cluster makes transformation of the blue dwarfs and red giants to the standard system straightforward. However, the photoelectric observations don't extend faint enough to include cool cluster dwarfs, a limitation which also impacts the calibration of $H\beta$, a point we will return to below.

For transformation to the standard system, the number and quality of the internal standards within NGC 752 are strongly dependent upon which filter(s) are being transformed. For V , as of 1994 (Daniel et al. 1994) there were 5 sources of V -equivalent data; that number has since grown to 8. For $wvby$ and $H\beta$, the sources have doubled to 4 and 2, respectively, while for $Caby$, only one source exists (Anthony-Twarog & Twarog 2006), supplying hk indices for 7 giants and 21 stars at the cluster turnoff.

For the color indices $b - y$, m_1 , c_1 , and $H\beta$, and the V magnitude, the photoelectric data from all available sources, unless otherwise noted, were merged after applying appropriate zero-point corrections and weighting by the inverse squares of the standard error of the mean for the individual data points. Extensive discussion of an earlier attempt to merge the myriad photometric data sets for NGC 752, including Strömrgren photometry, can be found in Daniel et al. (1994), but the analyses of Joner & Taylor (1995) and Taylor, Joner, & Jeffery (2008) emphasize a precision match to the zero-points for the fundamental $wvbyH\beta$ and V systems, so we will present a revised merger of each of the indices and V .

Prior to initiating the merger, a note on cluster identifications is necessary. As is common with well-studied open clusters, NGC 752 has accumulated an extensive list of numbering systems over the years, 12 as of this writing. The most comprehensive is that defined by WEBDA; the most recognizable in past discussions of the cluster is that of Heinemann (1926). When identifying stars in the discussions below, we will default to the Heinemann (1926) (H) number, placing the WEBDA number in parentheses after the H number if they differ. Thus, if only the H number

is supplied, it is assumed that the WEBDA and H numbers are the same. If a star has no H identification, only the WEBDA number will be supplied, preceded by W.

For $H\beta$ only two data sources are available, Crawford & Barnes (1970) and Joner & Taylor (1995). An increase of 0.008 mag was applied to the unevolved stars of Crawford & Barnes (1970), based upon a comparison of 12 turnoff stars common to the two data sets, and the sets merged. Crawford & Barnes (1970) also observed 4 red giants which have not been adjusted for the offset defined by the turnoff stars. The final list of 40 potential $H\beta$ standards ranges from 2.566 to 2.919.

For $b-y$, m_1 and c_1 , we have data from Crawford & Barnes (1970); Twarog (1983); Joner & Taylor (1995) and Anthony-Twarog & Twarog (2006), though the last source supplies m_1 and c_1 solely for the 7 giants. For c_1 , the systems of Crawford & Barnes (1970) and Joner & Taylor (1995) are virtually identical; an offset of -0.001 was applied to the c_1 indices of Crawford & Barnes (1970) and the data merged. From 17 stars common with the merged sample, an offset of -0.010 ± 0.009 (sd) was found and applied to the c_1 data of Twarog (1983). Only Crawford & Barnes (1970) included red giants in their photometry and, while an offset of -0.010 in c_1 was also found, the overlap of 3 stars with Anthony-Twarog & Twarog (2006) was considered too small to provide a reliable offset, so the photometry was left unchanged. Lastly, one bright G star was observed as part of the catalog of Olsen (1993). Since our cool-star *uvby* standards are tied to this catalog, the star, H39, has been added to the standard list without change. All adjusted c_1 data were sorted and merged with weights tied to the inverse squares of the standard error of the mean for each star, leading to 46 potential c_1 standards.

Identical procedures were followed for m_1 and $b-y$. No offset exists in m_1 or $b-y$ for the photometry of Crawford & Barnes (1970) and Joner & Taylor (1995). The derived adjustments from 17 stars for Twarog (1983) were $+0.013 \pm 0.011$ (sd) and $+0.002 \pm 0.007$ (sd) for m_1 and $b-y$, respectively. For Anthony-Twarog & Twarog (2006), the m_1 indices for the giants remained unchanged but the $b-y$ indices for 20 dwarfs implied a correction of -0.009 ± 0.009 (sd). The one star from Olsen (1993) was added without adjustment. The adjusted indices were again merged and weighted by the inverse squares of the standard error of the mean, producing 46 potential m_1 standards and 47 $b-y$ standards; H192 has only been observed by Anthony-Twarog & Twarog (2006) and H235 has been excluded as a variable.

For V , Crawford & Barnes (1970) did not provide magnitudes. However, we attempted to merge the data of Johnson (1953); Eggen (1963); Jennens & Helfer (1975); Rufener (1981, 1988); Dzérvítis & Paupers (1993); Joner & Taylor (1995); Bartašūite et al. (2007). The V magnitudes of Dzérvítis & Paupers (1993) were eliminated after a number of stars exhibited unusually large residuals compared to multiple observations from other sources which showed no evidence for variability among these stars. Known variables H219 and H235 were excluded from the merger process.

For each source of photometry, residuals relative to Taylor, Joner, & Jeffery (2008) were calculated and a color term was tested for statistical significance. The resulting coefficients, zero-points, and final residuals after adjustment are presented in Table 1. The revised magnitudes for all sources

except Eggen (1963), due to the larger than average scatter, were merged and combined. Stars for which the residual from the mean relation exceeded three sigma for the specific comparison were excluded from the derivation of the adjustment and from the final average for the star; these stars are identified by H number in the final column of Table 1. For Rufener (1981, 1988), the standard error of the mean for the merger process was set at 0.010 mag for all stars. The final merged database included 150 potential V standards within the field of NGC 752.

Table 2 contains the final merged photoelectric photometry for all NGC 752 non-variable stars with any indices on the extended Strömgren and/or $H\beta$ systems. These data form the primary calibration standards within NGC 752. Stars with only V magnitudes are not included within the Table.

2.3. Internal Cluster Standards - Cool Dwarfs

As noted earlier, none of the stars listed within Table 2 is classified as a cool dwarf. To allow transformation of the faintest cluster members to the standard system, the CCD frames for NGC 752 from the Nov. 2010 run were treated as program frames and recalibrated with aperture photometry, with an emphasis on the cooler dwarfs within the cluster field, i.e. dwarf stars too bright to be cluster members but bright enough to have adequate photometric precision to define the slopes and color terms for the indices of interest. This particular run was chosen because it had the largest number of photometric nights with tie-ins to the cool dwarf field star standards.

Our calibrations to the standard extended Strömgren system are based on aperture photometry of field star standards and of stars in NGC 752 for each photometric night. For every frame contributing to the photometric calibration solution, aperture magnitudes for standard stars are obtained within apertures scaled to five times the full-width-half-maximum for the frame; sky annuli are uniformly chosen with the inner radius one pixel larger than the aperture and a uniform annular width. In addition to the stars of Table 2, a number of sources were consulted for field star standard indices, including the catalog of Twarog & Anthony-Twarog (1995) for V , $b-y$ and hk indices, catalogs of $uvbyH\beta$ observations by Olsen (1983, 1993, 1994), and compilations of $H\beta$ indices by Hauck & Mermilliod (1998) and Schuster & Nissen (1989).

While our emphasis for the Nov. 2010 run was on the cool dwarfs, calibration relations were derived for all indices, colors, and luminosity classes. A single $b-y$ calibration equation was derived for warmer dwarfs and giant stars, with a separate calibration equation for dwarfs with $b-y \geq 0.45$. Calibration slopes and color terms for m_1 and c_1 for cooler giants were determined independently from those for bluer dwarfs or cooler main sequence stars, with the condition that the final relations mesh at the color boundary; the zero points for all relations were set by the standards of Table 2. The final step of extending the secondary standards within NGC 752 to cooler dwarfs used the average differences between the merged profile-fit photometry and indices from the entire run and the standard indices defined from the aperture photometry to transfer the PSF indices to

the standard system. Since the shorter exposures in NGC 752 aren't exceptionally rich, crowding proved to be a non-issue and virtually every PSF star within the cluster frames could be translated to the standard system directly. The field star calibration relations for the cool giants and hotter dwarfs from the Nov. 2010 run proved to be completely consistent with the values derived using the internal photoelectric standards as calibrators, thereby supplying secondary CCD standards from hotter dwarfs and red giants stars not already observed photoelectrically. Due to the absence of cool dwarfs among the NGC 752 photoelectric standards, the secondary standards from the Nov. 2010 run for this group represent the primary, and potentially weakest, link to the standard system.

2.4. Variable Stars

Before initiating the calibration of all the instrumental indices to the standard system, a check was made for potential variables, stars whose colors and, especially, magnitudes could produce distortions in the transformation relations. Such stars, if cluster members, could also prove useful in identifying and explaining spectroscopic and/or photometric anomalies compared to normal stars within the CMD. While the CCD frames weren't obtained with a variable star search in mind, the large degree of field overlap within the mosaic of frames has produced both high precision and, for the cluster core stars brighter than $V \sim 15$, often more than a dozen observations each in b and y extending over a three-year period. Therefore, the search for variables was carried out in the following way. The mean standard deviations for a single observation in y and in b were calculated as a function of V for both the HDI and the S2KB photometry independently. Any star which exhibited photometric scatter in both y and b from the HDI data which was larger than 3.0 times the mean standard deviation at a given V was checked within the S2KB data. If the star was within the S2KB field and exhibited similar scatter, it was tagged as a probable variable. Stars in the HDI field with excessive scatter for which the comparison in the S2KB data was inconclusive, as well as HDI variables located outside the S2KB field, were classed as possible variables.

Our preliminary list contained 19 possible and 8 probable variables. As expected, the two well-studied cluster variables, H219 and H235, easily met all the criteria for probable variables. Each additional star was then checked for potential signs of PSF contamination from a nearby star (closer than $4''$) which could lead to apparent variability. This eliminated 2 probable variables and 5 possible variables, including one member, H182, a star we will see again in Sec. 3. Our final list totalled 6 probable variables and 14 possible variables brighter than $V = 17$. Proper-motion members among the probable variables are H58, H219, and H235, while possible variable members only include H129 and H156. H58 and H129 are noted as potential variables in Table 2.

2.5. Final Transformation Relations

For all indices and the V magnitude, a general calibration equation of the form

$$\text{INDEX}_{stand} = a_{index} * \text{INDEX}_{instr} + b_{index} * (b - y)_{instr} + c_{index}$$

was adopted. For V , $H\beta$, and hk , stars of all luminosity classes were treated initially as a group. For $b - y$, the sample was separated into two groups, cooler dwarfs or blue dwarfs/red giants. The optimal transition color for the separation was found to be $b - y = 0.46$. For m_1 and c_1 , calibration curves were attempted for three groups, blue dwarfs, red dwarfs, and red giants. The red giant photoelectric standards were supplemented by the secondary CCD standards when necessary, while the red dwarf calibrations are based exclusively on the internal CCD standards. The calibration coefficients, the number of stars used to define the relations, and the scatter among the residuals for each relation are presented in Table 3.

Of the 150 potential standards for V within the field of NGC 752, 116 fall within our CCD survey. Three of the newly identified potential variables (H58, H129, H170) within the CCD field were removed, leaving 113 stars. A preliminary calibration was tested and 8 additional stars were found to have larger than expected residuals. Once removed, the relation was rederived and the revised residuals tested for spatial variations across the CCD field using a quadratic function in both X and Y. It should be noted that the earlier merger between the S2KB and HDI data included spatially-dependent terms, but the adoption of the HDI frames as the true photometric system was partially arbitrary, leading to the need for a test of the HDI system with the photoelectric standards. The gradient in V residuals across the $42'$ field amounted to 0.02 mag, small but measurable given the precision of the instrumental magnitudes and the quality of the photoelectric standards. With application of a linear correction in X and Y, the final standard deviation in the residuals in V from 105 calibration stars is ± 0.010 mag.

Of the 8 stars with larger than expected residuals, the standard V magnitude for H135 is based upon an average from 5 sources with a standard deviation among the measures consistent with no variability. However, close examination of the CCD data reveals a fainter star within $3''$ of H135 which, if not excluded from the photoelectric flux, produces a V magnitude too bright by 0.06 mag, enough to explain the discrepancy within the photoelectric data. A virtually identical result is found for H309; the presence of a star 2.55 mag fainter within $3''$ of H309 leads to a photoelectric value too bright by 0.07 mag. H145 shows the largest discrepancy at 0.41 mag, with the sole observation from Taylor, Joner, & Jeffery (2008) being too bright. With more than 2 dozen observations each in b and y , our photometry for this star shows no indication of variability. As an independent check, the CCD V mag from the Vilnius survey of Bartašūiūtė et al. (2011) for H145 is 12.72, 0.39 mag fainter than that of Taylor, Joner, & Jeffery (2008). A possibility is that the star observed by Taylor, Joner, & Jeffery (2008) is H151, fainter and slightly redder than H145. A similar but less extreme discrepancy arises with H273. As noted earlier, comparison of the V data of Taylor, Joner, & Jeffery (2008) with that of Rufener (1981, 1988) led to elimination of this star from the merger of the latter data with the standard list since the V mag was too faint by 0.13 mag. Our data for this star exhibit the same offset while the Bartašūiūtė et al. (2011) CCD data show an offset of 0.12 mag. Based upon the V mag and very red color, we conclude that the star listed as H273 in Taylor, Joner, & Jeffery (2008) is possibly H272. H308 and H226 show no

variability and have no nearby faint companions; the Vilnius V magnitudes for these stars are in excellent agreement with ours, implying that the Rufener (1981, 1988) values are too bright by 0.15 and 0.07 mag, respectively. H100 is $9''$ from H99, a star 1.3 mag brighter and an easy source of contamination for a photoelectric measurement; Bartašūite et al. (2011) don't include this star in their survey. Finally, H176 is 0.04 mag fainter in our data than in Rufener (1981, 1988). There are no stars with V within 5 mag of the star within $20''$ of the star. The Vilnius V mag for the star lies midway between the two discrepant measures, i.e. within 0.02 mag of our final result.

For $H\beta$, the standard deviation of the residuals among the 39 nonvariable photoelectric standards within the CCD field is ± 0.007 mag. Given the precision of the photometry, the small dispersion would appear to validate the adoption of a single calibration relation for stars in all luminosity classes. However, a preliminary analysis of the cluster using $H\beta$ defined by such a relation produced identical well-defined trends of increasing metallicity with decreasing $H\beta$ for main sequence members using either hk or m_1 as the metallicity indicator. The similar trend from independently calibrated metallicity indices pointed to $H\beta$ as the common link to the problem, a result confirmed by a comparison to the metallicity obtained when hk and m_1 are analyzed as a function of $b - y$ rather than $H\beta$. The underlying basis of the problem is the narrow temperature range which defines the stellar sample within the vertical turnoff of NGC 752. Excluding the single blue straggler, the range in $H\beta$ is only 0.08 mag. The blue straggler expands this range to 0.27 mag, but the inclusion of the four red giants observed by Crawford & Barnes (1970) extends and defines the relation among the cooler stars. While the 34 turnoff stars set the definitive zero point for the $H\beta$ index, the trend of the residuals with $H\beta$ is set by the relative positions of the sole blue straggler and the red giants. A relation excluding the blue straggler but retaining the giants with the $H\beta$ of Crawford & Barnes (1970) corrected for the offset defined by the unevolved stars produces a linear relation with a statistically weak trend with $H\beta$, i.e. a slope near 1.0. If, as assumed in Table 2, the offset defined by the dwarfs doesn't apply to the red giants, the slope of the red giant calibration becomes 1.1. By contrast, dropping the giants but retaining the blue straggler creates a color dependence with a slope near 1.2.

For stars classified as dwarfs at all colors, we have adopted the $H\beta$ relation defined by the 35 unevolved stars. For the stars classified as giants, we will use the relation defined by the red giants without the offset (Joner & Taylor 1995) included. We will return to this point in Sec. 4 where the impact of the relation on both metallicity and reddening can be tested.

For hk , all 27 photoelectric standards are within the cluster field. One star, H259, exhibited larger than expected residuals and was dropped from the calibration. The remaining 26 stars produced a scatter of ± 0.023 , larger than the other Strömgren indices, but consistent with the significantly smaller number of photoelectric observations from only one source which were used to define the standard values.

For $b - y$, from 46 red giant/blue dwarfs (H135 excluded) with photoelectric measures, the scatter among the residuals about the mean relation was ± 0.005 mag, the same scatter found for

the cool dwarf relation defined by the 14 secondary CCD standards.

For m_1 , to delineate separate calibrations for cool dwarfs, blue dwarfs, and red giants, the primary standards from Table 1 were supplemented by the 14 red giant and 14 cool dwarf secondary CCD standards. From the red giant and blue dwarf relations, the 45 photoelectric standards of Table 1 (H135 excluded), exhibit a scatter about the mean relation of ± 0.009 mag. The secondary giant and dwarf standards show scatter of ± 0.017 mag and ± 0.020 , respectively, larger than for the photoelectric standards due to the more limited precision of the secondary CCD standards.

For c_1 , separate calibrations were attempted for the cool dwarfs, cool giants, and blue dwarfs but, within precision of the secondary CCD standards dominating the cool dwarf sample, the relations derived for the dwarfs were found to be the same, so both samples were merged to obtain the common relation. For the red giant relation, the 10 photoelectric standards of Table 2 were supplemented by 16 CCD secondary standards. One giant exhibited larger than expected residuals and was dropped from the calibration. The final scatter about the mean relation for the 45 photoelectric standards (blue dwarfs and red giants) is ± 0.019 mag. For the 14 cool dwarfs, the scatter among the residuals is ± 0.029 mag, larger than for the photoelectric standards, as expected.

Before discussing the analysis of the photometry, particularly the probable members of NGC 752, it would be useful to supply some insight into the classification of the cooler stars as giants or dwarfs. As explained above, this distinction is significant for the m_1 and c_1 indices and less so for $b - y$. For the study of clusters at greater distance, the dichotomy among cluster members is severely reduced since cooler dwarfs are often too faint to play an important role in the cluster analysis. For NGC 752, stars of approximately solar mass or lower have V magnitudes near 13 and fainter, well within the limits of the current study. Equally important, proper-motion membership is limited to stars brighter than $V \sim 15.5$, so identification of potential fainter members can be enhanced if field giants can be eliminated from the cooler sample.

For m_1 and c_1 , the most common means of separating giants from dwarfs for cooler stars ($b - y > 0.5$) has been the use of two-color diagrams, either m_1 or c_1 versus $b - y$ (see, e.g. Olsen (1984)) or combinations of these indices designed to enhance the separation, such as the LC parameter defined in Twarog, Vargas, & Anthony-Twarog (2007). Two issues arise in the application of these approaches: (a) for the coolest stars, $b - y > 0.7$, the separation of the indices between dwarfs and evolved stars decreases with increasing color and (b) the luminosity distinction must be made using instrumental indices prior to application of the often distinctly different calibration curves for each class. A practical alternative is supplied by the hk and $H\beta$ indices which traditionally do not require separate calibration curves based on luminosity class. As detailed in Twarog & Anthony-Twarog (1995), the $hk - (b - y)$ relations for evolved and unevolved stars separate near $b - y \sim 0.5$, with the separation increasing until $b - y \sim 0.7$, where the dwarf relation reverses and hk declines with increasing $b - y$, crossing the evolved star trend near $b - y = 0.8$ but growing more disparate with increasing $b - y$. This pattern is illustrated in Fig. 1, where stars classed as unevolved and evolved are plotted as open and filled circles, respectively. The sample is composed of all

stars with V brighter than 16.0 with at least 3 observations in each filter and final photometric errors below 0.015 in $b - y$ and 0.030 in hk . For the region near $b - y = 0.75$ and beyond, a second criterion has been adopted to aid in distinguishing evolved stars from dwarfs. As detailed in Twarog, Vargas, & Anthony-Twarog (2007), $H\beta$ loses sensitivity for cool giants, approaching a value near 2.55 defined by the relative width of the $H\beta$ filters. By contrast, for dwarfs, $H\beta$ continues to decline as $b - y$ increases, reaching a minimum near 2.48 before reversing the trend with increasing color. The pattern is illustrated in Fig. 2, where the stars are limited to those with errors in $H\beta$ below 0.020. The symbols have the same meaning as in Fig. 1. It should be emphasized that while the final calibration for $H\beta$ has included a distinction between giants and dwarfs for reasons noted earlier, use of a common relation for both classes leaves the pattern of Fig. 2 unchanged. The $H\beta$ scale becomes slightly compressed with the giants hitting a limit at 2.56 instead of 2.55 and the dwarfs minimized at 2.50 instead of 2.485.

Some confusion of classification does occur, typically for the bluest stars for which the separation in Fig. 1 is least reliable and photometric scatter can easily lead to misclassification. Fortunately, the differences in the final indices caused by selecting the wrong calibration are also severely reduced in this color regime. For fainter stars without reliable hk or $H\beta$, the dwarf classification has been adopted by default.

Final photometry on the $uvbyCaH\beta$ system can be found in Table 4, where stars are sorted by magnitude and identified primarily by right ascension and declination (J2000.00), with CCD coordinates transferred to the system of Høg et al. (2000). The sequential photometry columns are V , $b - y$, m_1 , c_1 , hk , and $H\beta$, followed by the standard error of the mean in each index and the number of frames included for y , b , v , u , Ca , $H\beta$ narrow, and $H\beta$ wide. The identification sequence is WEBDA(W), PL, Heinemann (1926)(H), Rohlfis & Vanysek (1961)(RV), and Stock (1985)(ST). The last two columns are the membership probability from PL, if available, and the classification used to define the calibration relations. Stars without membership data are assigned -1. Photometry has been included only if a star has been observed twice within each filter used to construct the magnitude/color index and the final errors in the magnitude/color index fall below 0.050 for V and $H\beta$, 0.070 for $b - y$, 0.075 for m_1 and c_1 , and 0.10 for hk . A plot of the standard errors of the mean as a function of V for V and the five color indices is shown in Fig. 3. At $V = 16$, the typical standard errors of the mean are 0.010 mag for $b - y$, 0.015 mag for m_1 and $H\beta$, and just under 0.020 mag for hk and c_1 .

3. The Color-Magnitude Diagram

The CMD based upon $(V, b - y)$ for all stars in Table 4 is shown in Fig. 4. Stars for which the internal errors in $b - y$ are below 0.015 mag are plotted as open circles. While the probable location of the cluster CMD, particularly the giant branch, is discernible, the majority of stars within the CCD field are definitely nonmembers, especially below $V = 15$. To reduce the confusion, a first cut is made based upon the proper-motion survey of PL. Of 175 stars with non-zero membership

probability, 124 lie within the CCD field.

The second cut uses the radial-velocity measures of Daniel et al. (1994); Mermilliod et al. (2008, 2009); Maderak et al. (2013). Stars H177, H186, and H258, for which multiple radial-velocity measures showed no evidence for variability but a mean value significantly different from the cluster, were excluded as nonmembers. H64 is classed as a questionable member based upon radial-velocity measurements (Mermilliod et al. 2009); it has been excluded from the sample. The 120 remaining stars are plotted in Fig. 5. Open black circles are all dwarfs for which only proper-motion membership is available. Filled black circles are dwarfs with both proper-motion and radial-velocity membership, but too few radial velocities, usually one, to test for variability. One star with multiple radial-velocity measures but a large uncertainty in the final velocity due to rotational broadening of the spectral lines, H159, is plotted as a filled black circle. Filled red circles (triangles) are stars where multiple radial-velocity measures are consistent with membership and single-star status. Filled blue circles (triangles) are stars where multiple radial-velocity measures are consistent with membership and binarity. Two of the stars classed as radial-velocity nonmembers by Maderak et al. (2013) based upon a single velocity measurement (P552, P828) are known single-lined spectroscopic dwarfs and are plotted as such. Four dwarfs have single radial-velocity measures from Maderak et al. (2013) which deviate significantly from the cluster mean, implying they could be nonmembers and/or binaries. These are plotted as green stars. P964 (H244) is a radial-velocity member with no evidence for binarity according to Daniel et al. (1994) and Mermilliod et al. (2009); Maderak et al. (2013) identify it as a nonmember based upon a single deviant measure. We have plotted it as a single-star member.

While the cluster CMD is now extremely well-delineated, deficiencies in our categorization of the stars still remain. The stars for which only proper-motion membership is available fall into two categories. At the faint end, where the membership probabilities approach single digits, the four bluest stars between $V = 14$ and 15.5 are highly probable nonmembers, background dwarfs whose proper-motion uncertainties place them marginally within the range of the cluster. Another six appear to lie on the main sequence, while a seventh would need to be a binary based upon the position in the CMD. We will return to these below. Surprisingly, the second group of stars with minimal information includes 8 stars which populate the red hook at the top of the main sequence at $V = 10.5$ or brighter. Because of their apparent brightness relative to the field, it is almost certain that these stars would be confirmed as members if radial-velocity data were available. Their importance lies in the fact that almost all stars bracketing this region of the CMD are classed as binaries. If single stars, given that these are the approximate progenitors of the red giants, a more comprehensive investigation of their physical state could shed significant light on the confusing mix of abundances for Li and CNO found among the giants (Anthony-Twarog et al. 2009; Böcek Topcu et al. 2015).

Moving down the main sequence, with the exception of the highly probable faint nonmembers, three stars appear to sit slightly blueward of the main sequence. The single-star member near $V = 12.3$ is H182, originally tagged as a potential variable from the scatter in the photometry but

now believed to suffer from contamination by a nearby fainter star, thus explaining its odd position in the CMD. Two low-probability members, W6341 (proper-motion membership probability = 2%) and W7384 (1%), without radial-velocity information at $V \sim 14.75$ comprise the rest of the probable blue CMD deviants. Three of the four stars plotted as starred points due to a deviant single radial-velocity measure (Maderak et al. 2013) fall above the main sequence. One of these (H90, 23%) appears to be too bright to be a binary member of the cluster and is photometrically classed as a giant. A similar classification befalls the brightest of the green stars, making both of these highly likely nonmembers. H156 (87%) is classed as dwarf but has a position in the CMD which is marginally too bright to be within the cluster. Only the faintest green star is both a dwarf and within the confines of the cluster CMD. Finally, the reddest star in the plot at $V \sim 12.4$ is classed photometrically as a field red giant.

As an independent means of identifying potential nonmembers through an anomalous CMD position, we turn to the $V - hk$ diagram of Fig. 6. hk has the advantage of being more sensitive to changes in temperature than $b - y$ while remaining relatively insensitive to reddening. Equally important, increased reddening in $b - y$ moves hk toward lower/bluer values; $Ehk = -0.16^*E(b - y)$. Symbols in Fig. 6 carry the same meaning as in Fig. 5; the four stars with $b - y$ less than 0.50 located well below the main sequence of Figure 5 have been excluded from the figure and will not be discussed further. In Fig. 6, 2 stars immediately stand out by lying below the main sequence near $V = 14.75$; these two stars are W6341 and W7384, also tagged for lying blueward of the main sequence in Fig. 5. All other stars have positions on or above the main sequence, but a closer analysis reveals that while the sequence of points with increasing $b - y$ should map to a similar sequence with increasing hk , some stars have hk indices which are inconsistent with their order in $b - y$. A trivial example comes from the reddest star on the lower main sequence, W496 (1%), located in a position in Fig. 5 which would imply that it must be a binary. However, in Fig. 6 this star is located at a much bluer color, placing it on the expected single-star main sequence. Equally anomalous are two filled circles (H69, H159) in the turnoff region which lie significantly redward of the main sequence hook, almost within the subgiant region, while remaining blueward of this boundary in Fig. 5.

The color sequence discrepancies are readily apparent in Fig. 7, where $b - y$ is plotted relative to hk for unevolved stars. A well-defined trend delineates the cluster main sequence, but a few points stand out. The blue point above the relation at $b - y = 0.34$ is H235, an eclipsing binary with a significant scatter in all indices. The three discrepant points redward of the relation between $hk = 0.55$ and 0.65 are H182, H69, and H159. H182 is the likely contaminated star which was too blue in $b - y$; making $b - y$ too small should lead to hk being too large, as observed. As noted earlier, H69 is a radial-velocity member based on only one measurement (Mermilliod et al. 2009), making it impossible to determine if this star is a possible binary. H159 has a radial velocity consistent with membership from multiple observations, but the uncertainty in the final value is indeterminate due to the apparently high rotation rate for the star. Its position well above the red hook would make a binary nature highly plausible, but its position could be tied to its high rotation rate, following

the arguments of Brandt & Huang (2015) that rapid rotators at a given age are longer-lived stars of higher mass which should appear brighter than slower rotators. Moving toward the redder stars, the single-lined spectroscopic binary H313 is the deviant point above the relation near $hk = 0.7$. The deviant open circle at $hk = 1.0$ is the previously tagged, low probability member W6341. The anomalous position of the projected lower main sequence binary now becomes apparent at $hk = 1.3$. Finally, the green, starred points all lie above the mean relation, indicating they are too blue in hk for their $b - y$ colors, adding credence to the radial-velocity classification as nonmembers. Only the reddest of the starred points is marginally consistent with photometric membership.

4. Cluster Parameters

4.1. Reddening and Metallicity

Given the extensive and growing literature on NGC 752, the primary purpose of this study is not a comprehensive rediscussion of the cluster reddening and metallicity. However, a strength of the extended Strömgren system is the ability to supply precise reddening and metallicity for individual stars, the latter from two independent indices, m_1 and hk , with optimal sensitivity for F dwarfs, the exact range covered by the stars at the turnoff of NGC 752 and extending to $V \sim 13$. Fig. 8 illustrates the pattern between $b - y$ and $H\beta$ for all possible proper-motion members, excluding the faint blue probable nonmembers below the main sequence in Fig. 5 and the one blue straggler at $(H\beta, b - y) = (2.931, 0.016)$. Since $H\beta$ is reddening independent, the vertical scatter in $b - y$ has two dominant sources, photometric error and reddening. Among the brighter stars, excluding a handful of deviant points, the standard deviation in $b - y$ at a given $H\beta$ is below ± 0.011 mag. A photometric scatter in $H\beta$ of ± 0.008 alone would explain this. Note also that there is no evidence for separation of the sample into binaries and single stars so elimination of binaries would reduce the final precision without altering the cluster mean. We conclude that there is no evidence for reddening variation across the cluster face, not surprising for a cluster with $(m - M) = 8.4$.

Among the hotter stars, the two most deviant points are the usual suspects, the eclipsing binary H235 (filled blue circle) on the high $b - y$ side and H182 (filled red circle) on the low $b - y$ side. Of the seven open circles (only proper-motion membership available) three fall on the low side of the mean relation. Whether or not this is significant must await spectroscopic observations of these stars.

At the redder end of the sample, the cluster red giants emerge, following the same pattern laid out in Fig. 2, with a lower limit of 2.55 to $H\beta$ at increasing $b - y$. Among the potential lower main sequence stars, there is an apparent shift to larger $b - y$ among many of the stars with $H\beta$ less than 2.57. Based upon the pattern illustrated in Fig. 2 and the location of the cluster red giants in this figure, we conclude that many of the stars with low proper-motion membership at the base of the main sequence are evolved background stars. This conclusion has already been confirmed for the two bluest starred points. Among the deviants points sitting between the dwarfs and the giants

is W6341 again, making it an anomaly in every diagram studied and a likely evolved background field star.

As we have done consistently in our cluster work, we will derive the reddening from two Strömgren relations from Olsen (1988) and Nissen (1988), a slightly modified version of the original relations derived by Crawford (1975, 1979). Reddening estimates are derived in an iterative fashion. The indices are corrected using an initial guess at the cluster reddening and the intrinsic $b - y$ is derived using the reddening-free $H\beta$ adjusted for metallicity and evolutionary state. A new reddening is derived by comparing the observed and intrinsic colors and the procedure repeated. The reddening estimate invariably converges after 2-3 iterations. To derive the reddening, one needs to correct $b - y$ for metallicity, so a fixed $[\text{Fe}/\text{H}]$ is adopted for the cluster and the reddening derived under a range of $[\text{Fe}/\text{H}]$ assumptions that bracket the final value. The complementary procedure is to vary the mean reddening value for the cluster and derive the mean $[\text{Fe}/\text{H}]$. Ultimately, only one combination of $E(b - y)$ and $[\text{Fe}/\text{H}]$ will be consistent.

The sample for metallicity and reddening estimation consists of 68 stars out of an original sample of 74. We have eliminated the deviants identified in Fig. 7, as well as H193 and the variable H219. H193 is classified as an Fm star (Garrison 1972), leading to $[\text{Fe}/\text{H}] = +0.7$ from m_1 . $[\text{Fe}/\text{H}]$ from hk is consistent with the cluster mean, but it will be excluded from both averages. Two additional stars classified as possible Fm stars, H58 and H234, generate metallicities consistent with the cluster mean and have been retained. For NGC 752, the metallicity defined by m_1 was varied between $[\text{Fe}/\text{H}] = -0.30$ and $+0.30$, generating a range of $E(b - y) = 0.030$ to 0.020 for the relation of Nissen (1988) and 0.030 to 0.016 for Olsen (1988) from 68 stars; in all cases, the standard deviation of a single measurement is only ± 0.011 mag. The slightly higher reddening for F stars using the Nissen (1988) relation compared to that of Olsen (1988) is a consistent occurrence from such comparisons (Carraro et al. 2011; Anthony-Twarog et al. 2014).

With $E(b - y)$ set at a range of values between 0.020 and 0.030 , $[\text{Fe}/\text{H}]$ has been derived from both m_1 and hk , using $H\beta$ as the primary color index. The best fit for simultaneous reddening and metallicity from m_1 produces $E(b - y) = 0.025 \pm 0.003$, where the uncertainty is totally dominated by the systematics of the intrinsic color relations and based upon one-half the difference between the two values. If $E(B - V) = 0.73 * E(b - y)$, the reddening estimate from Strömgren data alone is $E(B - V) = 0.034 \pm 0.004$. The final $[\text{Fe}/\text{H}]$ from 68 stars is -0.071 ± 0.014 (sem) and -0.017 ± 0.008 (sem) from m_1 and hk , respectively. In contrast with our preliminary analysis using a common slope for calibration of $H\beta$, a plot of the individual abundances as a function of $H\beta$ in Fig. 9 shows no trend with decreasing $H\beta$ for either m_1 or hk . The standard deviation in $[\text{Fe}/\text{H}]$ from hk is noticeably smaller than that from m_1 , a reflection of the greater metallicity sensitivity of hk over m_1 for F dwarfs. By contrast, the dispersion becomes comparable for the two indices near the boundary of the early G stars, illustrating that at cooler temperatures, the m_1 and hk indices undergo significant increases with decreasing temperature, making the metallicity indices very sensitive to small changes in $H\beta$, and generally less reliable indicators of $[\text{Fe}/\text{H}]$ (Twarog & Anthony-Twarog 1995; Anthony-Twarog, Twarog, & Yu 2002; Twarog, Vargas, & Anthony-Twarog 2007).

Both the reddening estimate and the metallicity are in excellent agreement with the most recent work on the cluster. The definitive discussion of the reddening is that of Taylor (2007) where the adopted value becomes $E(B - V) = 0.044 \pm 0.003$. The most recent high-dispersion spectroscopy by Böcek Topcu et al. (2015) of 10 red giants leads to $[\text{Fe}/\text{H}] = -0.02 \pm 0.05$ while Maderak et al. (2013) derive $[\text{Fe}/\text{H}] = -0.063 \pm 0.013$ from 36 main sequence stars, adopting $E(B - V) = 0.035$. More complete discussions of all previous spectroscopic work can be found in these papers.

4.2. Extending the Main Sequence

While the proximity of a star cluster theoretically supplies access to a homogeneous sample of low mass stars, for objects like NGC 752 and Rup 147, the greater age and low stellar density can mean that the few stars which remain bound to the cluster can easily be lost in the confusion of a rich background field. As demonstrated in previous sections, many of the lower probability, proper-motion members fainter than $V = 14$ have indices and CMD positions incompatible with membership in NGC 752. Identification of photometric members fainter than $V = 14$ has been attempted by Bartašūiė et al. (2011) using Stromvil indices and CMD location. Between $V = 15$ and 16.5, they identify 12 potential photometric members.

While the precision of the indices varies as a function of location in the field due to the partially overlapping mosaic of frames, the $V, (b - y)$ combination remains reliable for almost all stars down to at least $V = 16.5$. In an effort to identify potential cluster members, we have selected all stars with V between 15.0 and 16.5 and $b - y$ greater than 0.5 with photometric errors in $b - y$, $H\beta$ and hk below 0.015, 0.020, and 0.030 mag, respectively. These stars were plotted in the CMD and the cluster main sequence from known members above $V = 15$ was extended. Any star which deviated from the probable main sequence by more than 0.020 mag in $b - y$ on the blue side was eliminated. On the red side, stars were kept if they fell within 0.6 mag in V of the projected unevolved main sequence. Stars were then checked to see if their indices classified them as dwarfs or evolved stars. Of the 12 stars tagged as photometric members by Bartašūiė et al. (2011), eight met all of our precision criteria. Of these, six are confirmed as probable members (W6878, W6932, W6962, W7010, W7311, W7578), while two are excluded (W7176, W7390). The remaining four were initially excluded due to larger errors in hk and/or $H\beta$. Of these, from $V, (b - y)$ alone, W7274 is a probable nonmember, while W7039, W7187, and W7346 are consistent with main sequence stars. W7039 presents a special case. Its $hk, (b - y)$ position in Fig. 1 clearly places it among the dwarf sample. However, its location in the $H\beta - (b - y)$ plot (Fig. 2) classified it as a giant, so it was calibrated as a giant. If we require it to be a dwarf and apply the dwarf calibration for $b - y$, the final color shifts 0.04 mag to the blue, making this star inconsistent with cluster membership. It has been eliminated from the membership discussion. From outside the survey area of Bartašūiė et al. (2011) 16 stars have been identified as probable members; their WEBDA identifications are 6415, 6476, 6516, 6528, 6559, 6628, 6766, 6795, 6845, 6891, 7022, 7132, 7156, 7267, 7537, and 7669. We emphasize again that some of these stars are located above the unevolved

main sequence in a position indicative of binarity, if they are members. The CMD of the selection is shown in Fig. 10. Symbols have the same meaning as in Fig. 5, with the following additions: open black squares are the 16 probable members from our data alone, open blue squares are the members in common with Bartašūite et al. (2011), blue crosses are the photometric members of Bartašūite et al. (2011) which we classify as nonmembers, red crosses are the stars identified as nonmembers from our data alone, and green crosses are stars which lie on/near the main sequence but have indices which classify them as evolved stars.

4.3. Distance and Age

One of the rare sets of available isochrones which include models transformed to the Strömgren system is the Victoria-Regina (VR) set of isochrones (VandenBerg, Bergbusch, & Dowler 2006). Fig. 11 shows the scaled-solar models for $[\text{Fe}/\text{H}] = -0.04$, ages 1.3, 1.4, and 1.5 Gyr, adjusted for $E(b - y) = 0.025$ and $(m - M) = 8.30$. All stars classed as binaries and/or likely nonmembers, as discussed in previous sections, have been eliminated. Symbols have the same meaning as in Figs. 5 and 10. Keeping in mind that no membership information beyond location in the CMD is available for the square points, the isochrones supply an exceptional match to the entire CMD with an adopted age of 1.45 ± 0.05 Gyr. For comparison, the analysis of Anthony-Twarog et al. (2009) using the composite broad-band BV data of Daniel et al. (1994) and the Demarque et al. (2004) (Y^2) isochrones with $[\text{Fe}/\text{H}] = -0.05$ and $E(B - V) = 0.035$ derived an age of 1.45 Gyr and $(m - M) = 8.4$. The slightly smaller modulus is within the uncertainties of the broad-band result. Bartašūite et al. (2011) use Vilnius photometry to derive $E(B - V) = 0.048$ and $[\text{Fe}/\text{H}] = -0.16$; from comparison to older Padova isochrones (Bressan et al. 1993; Fagotto et al. 1994), they find an age of 1.4 Gyr and an apparent modulus of $(m - M) = 8.38$.

5. Summary and Conclusions

With increasingly larger CCD cameras becoming the standard on telescopes of medium and large aperture, a challenge for many less traditional photometric systems is calibration to a standard system. Unlike the extensive networks of standards used to define all-sky photometry for broad-band systems, intermediate and narrow-band standards are often limited to brighter and/or single stars within the field. While there are thousands of stars observed on the extended Strömgren system, outside of star clusters these are predominantly brighter than $V \sim 9.5$. As an initial step to remedy this problem, a $42' \times 42'$ field centered on NGC 752 has been observed to $V = 16.5$, with precision better than 0.010 mag for all indices for the majority of stars to $V \sim 15$.

The proximity of NGC 752 ensures that even with a telescope of modest size it is possible to reach stars of late K spectral type, fainter than the current limit of radial-velocity and proper-motion surveys of the cluster. Using multicolor indices, membership has been tested for the faintest

stars with nonzero proper-motion probabilities from PL. As expected, a majority are identified as likely nonmembers. Fortunately, the precision of the data allows us to extend the probable main sequence to $V = 16.5$, identifying 24 possible members, single and binary, between $V = 15$ and 16.5. The 12 photometric members identified by Bartašūite et al. (2011) within the cluster core have been checked and we concur on likely membership for 8 of them. The 16 additional photometric members are outside the area of the Vilnius study.

Using the photometry contained within this sample alone, the fundamental parameters for NGC 752 are rederived. The cluster is found to have $E(b - y) = 0.025 \pm 0.003$ ($E(B - V) = 0.034 \pm 0.004$) and $[\text{Fe}/\text{H}] = -0.03 \pm 0.02$ from 68 F stars, using a weighted average from m_1 and hk . With a well-defined main sequence of predominantly single stars, the Strömgren CMD is exceptionally well matched by an age of 1.45 ± 0.05 and $(m - M) = 8.30$ for $[\text{Fe}/\text{H}] = -0.04$, in excellent agreement with recent work tied to broad-band data.

Despite the apparent brightness of the stars near the turnoff, some questions remain regarding membership and binarity for stars near and above the main sequence red hook, the stars which populate the red giant branch and clump. Two stars (H69, H159) with anomalous hk values could be either nonmembers or stars demonstrating the effects of rapid rotation, while the supposedly single star, H108, lies well above the hook where no normal star should be found. Finally, the one definitive blue straggler, H209, has never exhibited radial-velocity or photometric variability; its age from comparison to the VR isochrones is less than 0.1 Gyr.

The paper has been significantly improved by the valuable and thoughtful comments of an anonymous referee who justifiably insisted that we probe deeper into the metallicity trends identified in an earlier version of the manuscript. Extensive use was made of the WEBDA database maintained by E. Paunzen at the University of Vienna, Austria (<http://www.univie.ac.at/webda>). The filters used in the program were obtained by BJAT and BAT through NSF grant AST-0321247 to the University of Kansas. NSF support for this project was provided to BJAT and BAT through NSF grant AST-1211621, and to CPD through NSF grant AST-1211699.

REFERENCES

- Anthony-Twarog, B. J., Deliyannis, C. P., Rich, E., & Twarog, B. A. 2013, ApJ, 767, L19
- Anthony-Twarog, B. J., Deliyannis, C. P., & Twarog, B. A. 2014, AJ, 148, 151
- Anthony-Twarog, B. J., Deliyannis, C. P., Twarog, B. A., Croxall, K. V., & Cummings, J. 2009, AJ, 138, 1171
- Anthony-Twarog, B. J., Deliyannis, C. P., Twarog, B. A., Cummings, J. D., & Maderak, R. M. 2010, AJ, 139, 2034

- Anthony-Twarog, B. J., & Twarog, B. A. 2000, *AJ*, 119, 2282
- Anthony-Twarog, B. J., & Twarog, B. A. 2004, *AJ*, 127, 1000
- Anthony-Twarog, B. J., & Twarog, B. A. 2006, *PASP*, 118, 358
- Anthony-Twarog, B. J., Twarog, B. A., & Yu, J. 2002, *AJ*, 124, 389
- Bartašūište, S., Deveikis, V., Straižys, V., & Bogdanavičius, A. 2007, *Baltic Astronomy*, 16, 199
- Bartašūište, S., Janusz, R., Boyle, R. P., & Davis Philip, A. G. 2011, *Baltic Astronomy*, 20, 27
- Böcek Topcu, G., Afsar, M., Schaeuble, M., & Sneden, C. 2015, *MNRAS*, 446, 3562
- Brandt, T. D., & Huang, C. X. 2015, astro-ph arXiv:1504.04375v1
- Bressan, A., Fagotto, F., Bertelli, G., & Chiosi, C. 1993, *A&AS*, 100, 647
- Canterna, R., Geisler, D., Harris, H. C., Olszewski, E., & Schommer, R. 1986, *AJ*, 92, 79
- Carrera, R., & Pancino, E. 2011, *A&A*, 535, 30
- Carraro, G., Anthony-Twarog, B. J., Costa, E., Jones, B. J., & Twarog, B. A. 2011, *AJ*, 142, 127
- Crawford, D. L. 1975, *AJ*, 80, 955
- Crawford, D. L. 1979, *AJ*, 84, 1858
- Crawford, D. L., & Barnes, J. V. 1970, *AJ*, 75, 946
- Cummings, J. D., Deliyannis, C. P., Anthony-Twarog, B. J., Twarog, B. A., & Maderak, R. M. 2012, *AJ*, 144, 137
- Curtis, J. L., Wolfgang, A., Wright, J. T., Brewer, J. M., & Johnson, J. A. 2013, *AJ*, 145, 134
- Daniel, S. A., Latham, D. W., Mathieu, R. D., & Twarog, B. A. 1994, *PASP*, 106, 281
- Demarque, P., Woo, J. -H., Kim, Y. -C., & Yi, S. K. 2004, *ApJS*, 155, 667 (Y^2)
- Dzérvišis, U. & Paupers, O. 1993, *Ap&SS*, 199, 77
- Eggen, O. J. 1963, *ApJ*, 138, 356
- Fagotto, F., Bressan, A., Bertelli, G., & Chiosi, C. 1994, *A&AS*, 105, 29
- Francic, S. P. 1989, *AJ*, 98, 888
- Friel, E. D., & Janes, K. A. 1993, *A&A*, 267, 75
- Friel, E. D., Janes, K. A., Tavaréz, M., et al. 2002, *AJ*, 124, 2693

- Garrison, R. F. 1972, *ApJ*, 177, 653
- Hauck, B., & Mermilliod, M. 1998, *A&AS*, 129, 431
- Heinemann, K. 1926, *Astr. Nach.* 227, 193
- Høg, E., et al. 2000, *A&A*, 355, L27
- Janes, K. A. 1979, *ApJS*, 39, 135
- Jennens, P. A., & Helfer, H. L. 1975, *MNRAS*, 172, 681
- Johnson, H. L. 1953, *ApJ*, 177, 357
- Joner, M. D., & Taylor, B. J. 1995, *PASP*, 107, 351
- Lee-Brown, D. B., Anthony-Twarog, B. J., Deliyannis, C. P., Rich, E., & Twarog, B. A. 2014, *AJ*, 149, 121
- Maderak, R. M., Deliyannis, C. P., King, J. R., & Cummings, J. D. 2013, *AJ*, 146, 143
- Mermilliod, J.-C., Mathieu, R. D., Latham, D. W., & Mayor, M. 1998, *A&A*, 339, 423
- Mermilliod, J.-C., Mayor, M., & Udry, S. 2009, *A&A*, 485, 303
- Mermilliod, J.-C., Mayor, M., & Udry, S. 2009, *A&A*, 498, 949
- Nault, K. A., & Pilachowski, C. A. 2013, *AJ*, 146, 153
- Nissen, P. E. 1988, *AJ*, 199, 146
- Olsen, E. H. 1983, *A&AS*, 54, 55
- Olsen, E. H. 1984, *A&AS*, 57, 443
- Olsen, E. H. 1988, *A&A*, 189, 173
- Olsen, E. H. 1993, *A&AS*, 102, 89
- Olsen, E. H. 1994, *A&AS*, 106, 257
- Pilachowski, C. A., Saha, A., & Hobbs, L. M. 1988, *PASP*, 100, 474
- Platais, I. 1991, *A&A*, 87, 69 (PL)
- Reddy, A. B. S., Giridhar, S., & Lambert, D. L. 2012, *MNRAS*, 419, 1350
- Rohlf, K., & Vanysek, V. 1961, *Astr. Abh. Hambourg* Vol. No. 7 (RV)
- Rufener, F. 1981, *Geneva Photometric Catalog*, Observatoire de Geneve

- Rufener, F. 1988, Geneva Photometric Catalog, Observatoire de Geneve
- Schuster, W. J., & Nissen, P. E. 1989, *A&A*, 221, 65
- Sestito, P., Randich, S., & Pallavicini, R. 2004, *A&A*, 426, 809
- Stock, J. 1985, *Rev. Mexicana Astron. Astrofis.*, 11, 103 (ST)
- Taylor, B. J. 2007, *AJ*, 134, 934
- Taylor, B. J., Joner, M. D., & Jeffery, E. J. 2008, *ApJS*, 176, 262
- Twarog, B. A. 1983, *ApJ*, 267, 207
- Twarog, B. A., & Anthony-Twarog, B. J. 1995, *AJ*, 109, 2828
- Twarog, B. A., Ashman, K., & Anthony-Twarog, B. A. 1997, *AJ*, 114, 2556
- Twarog, B. A., Anthony-Twarog, B. J., & Vargas, L. C. 2007, *AJ*, 134, 1777
- VandenBerg, D. A., Bergbusch, P. A., & Dowler, P. D. 2006, *ApJS*, 162, 375
- Zdanavičius, J., Bartašūte, S., & Zdanavičius, K. 2010, *Baltic Astronomy*, 19, 35

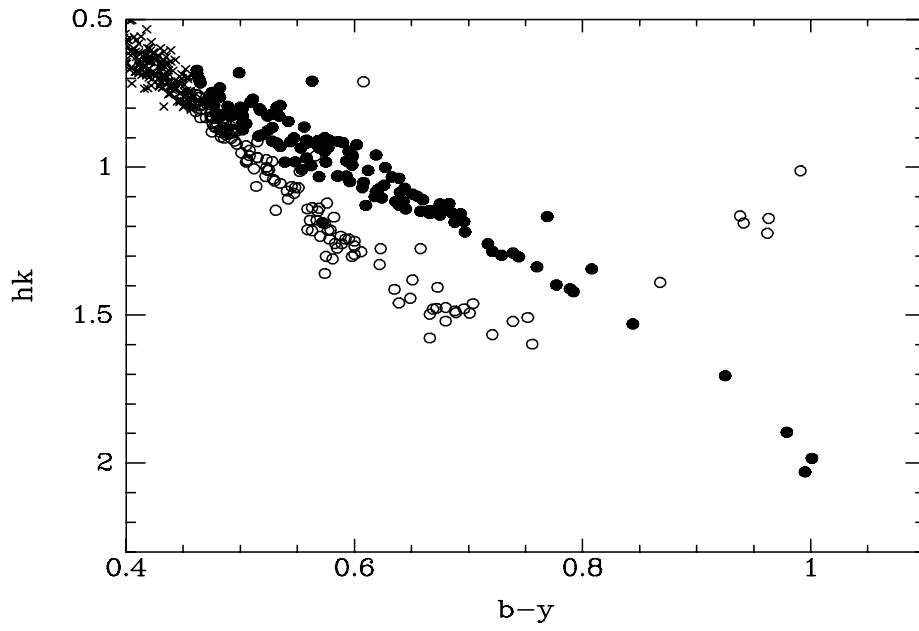


Fig. 1.— Using $hk - (b - y)$ to separate stars by luminosity class: stars classed as unevolved and evolved are plotted as open and filled circles, respectively. Crosses are stars for which no classification is possible.

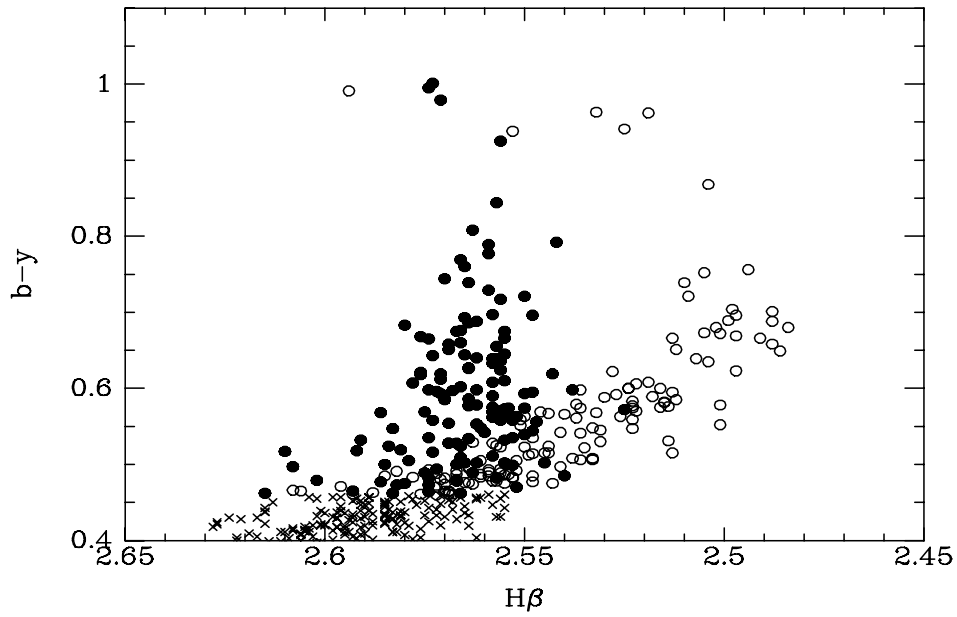


Fig. 2.— Same symbols as Figure 1, using $b - y$ versus $H\beta$ to separate stars by luminosity.

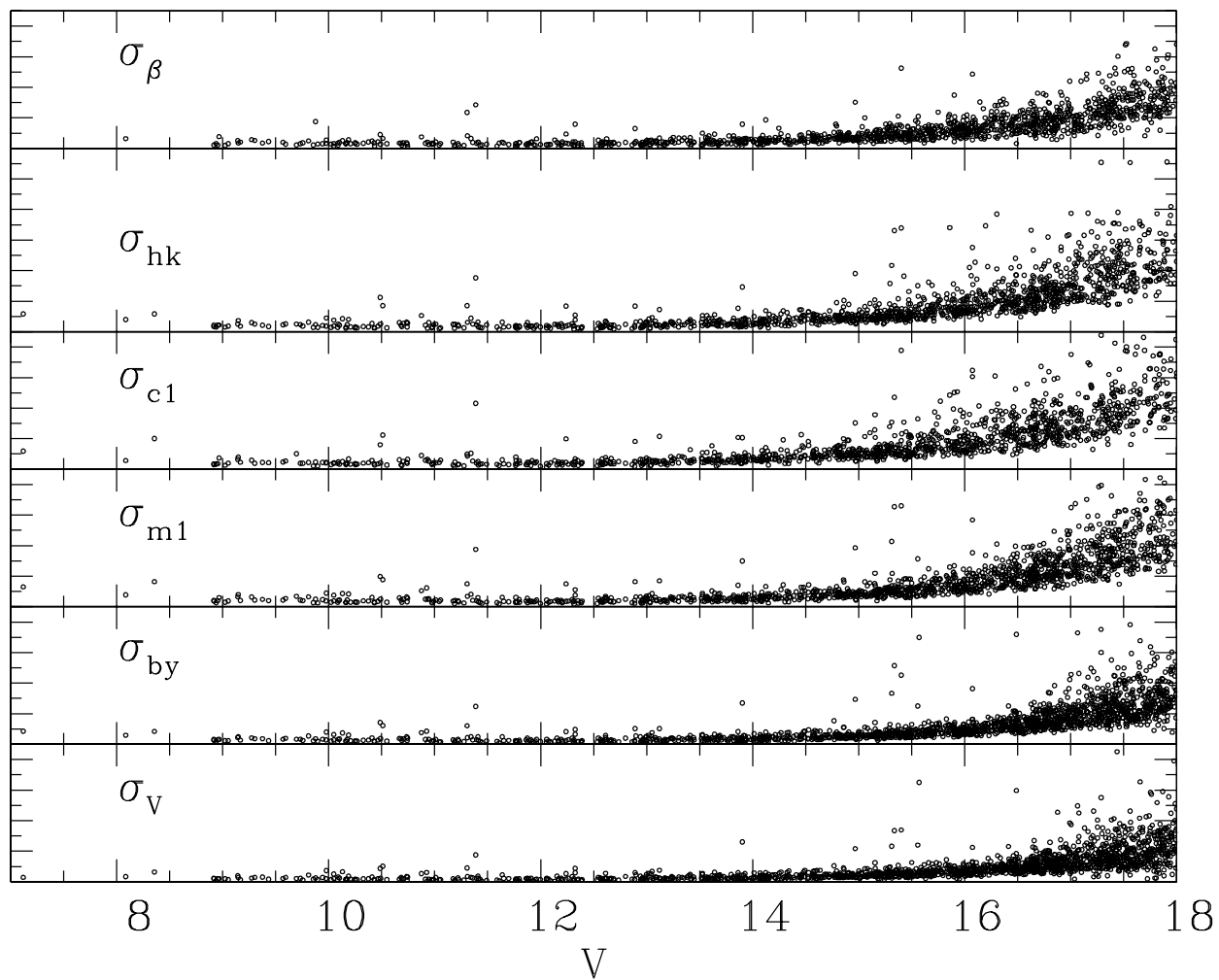


Fig. 3.— Average photometric errors in V , $(b - y)$, m_1 , c_1 , hk and $H\beta$ as a function of the V magnitude. The panel heights are scaled proportionately to the physical range, with major tick-marks indicative of 0.02 mag.

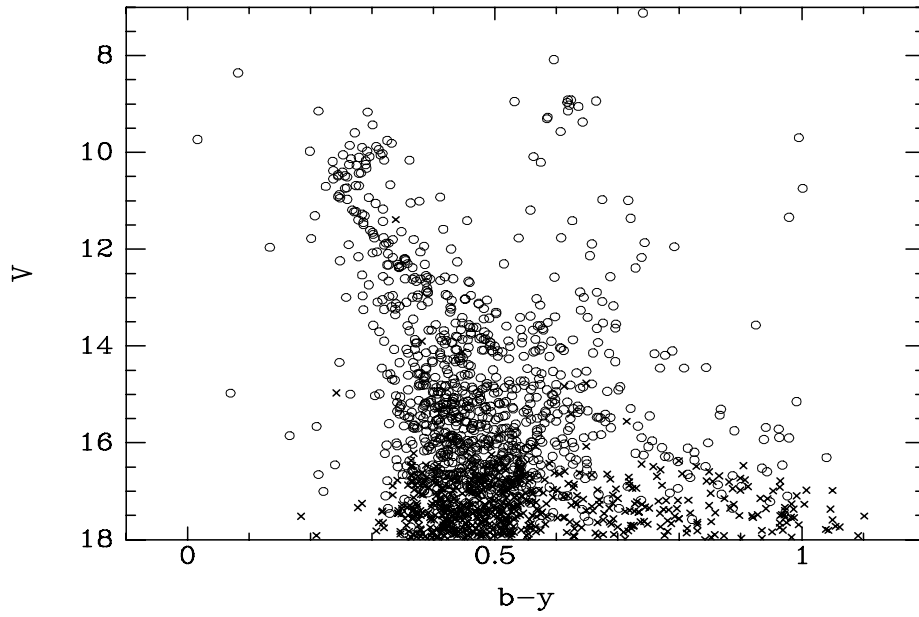


Fig. 4.— CMD for all stars in Table 4. Open circles are stars with photometric errors in $b - y \leq 0.015$. Crosses are stars with errors in $b - y$ larger than 0.015.

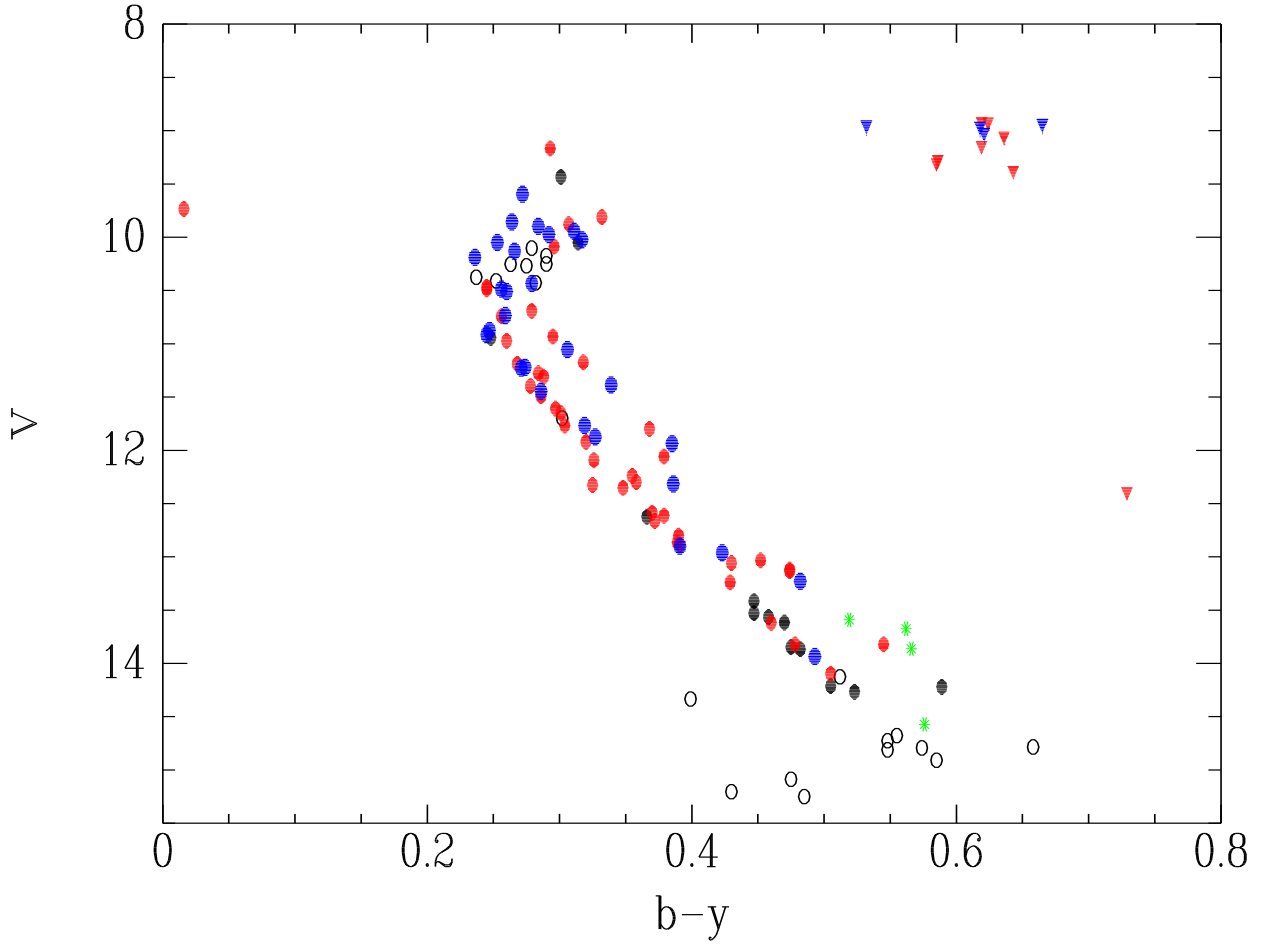


Fig. 5.— CMD of all stars with nonzero proper-motion membership probabilities. Open black circles are stars without radial velocities. Filled black circles are stars with radial-velocity membership, but too few to determine binarity. Filled red circles (triangles) are dwarf (giant) members without radial-velocity evidence for binarity. Filled blue circles (triangles) are dwarfs (giants) classed as member binaries. Four dwarfs with single radial-velocity measures which deviate significantly from the cluster mean, implying they could be nonmembers and/or binaries, are plotted as green stars.

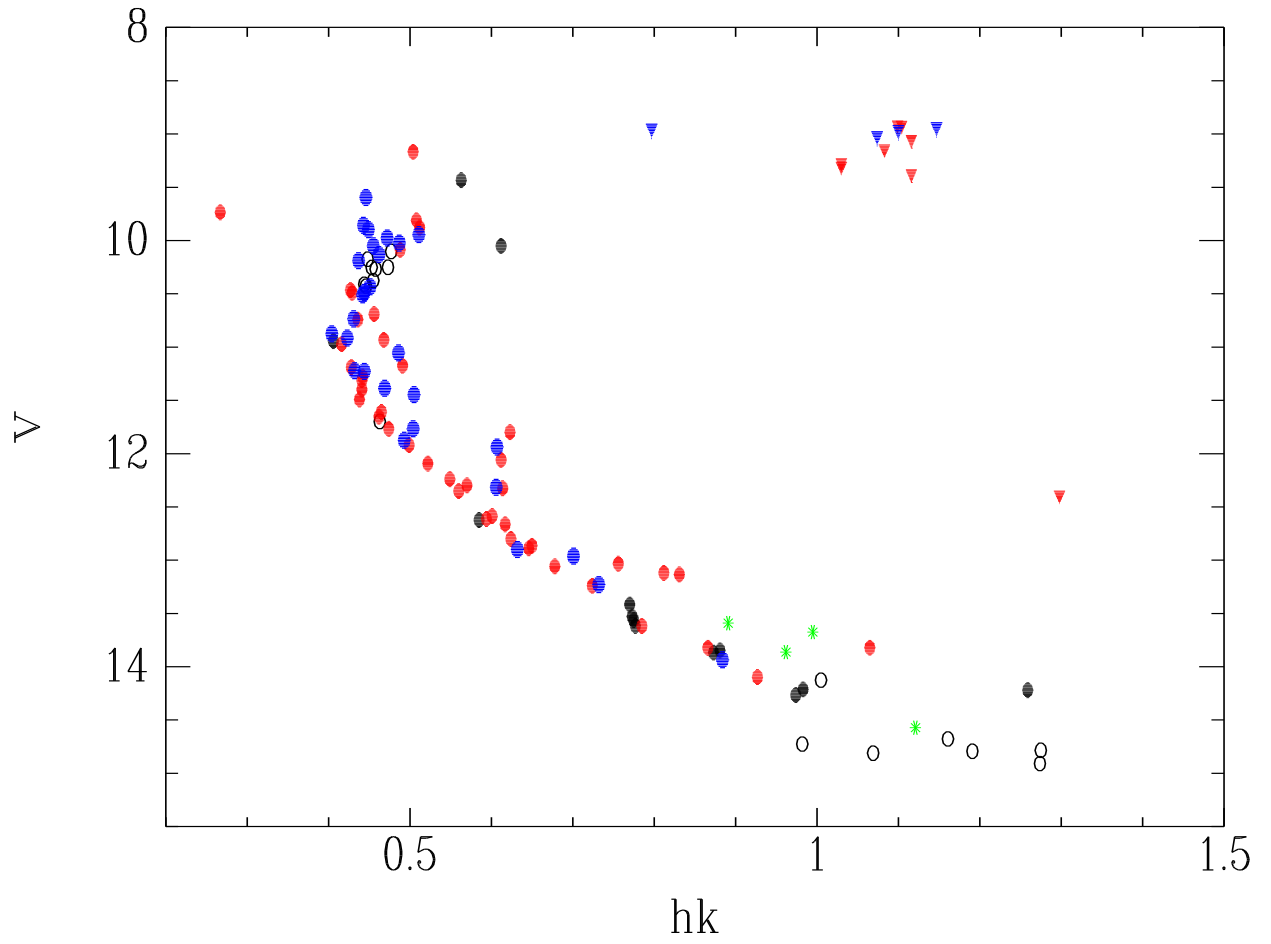


Fig. 6.— CMD based upon hk as the temperature index. Symbols have the same meaning as in Fig. 5.

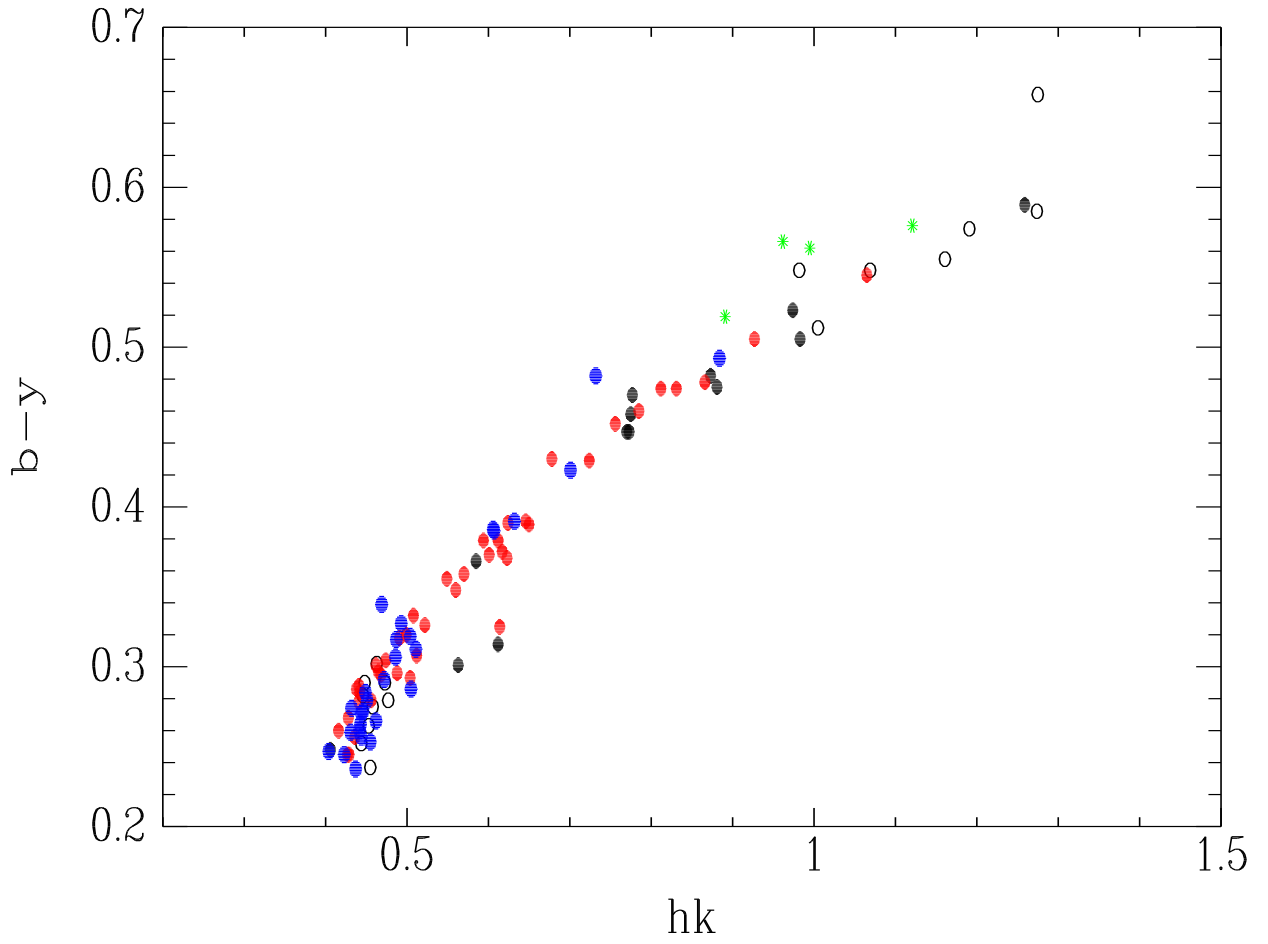


Fig. 7.— Color-color relation for the non-red-giant stars of Fig. 6. Symbols have the same meaning as Fig. 5.

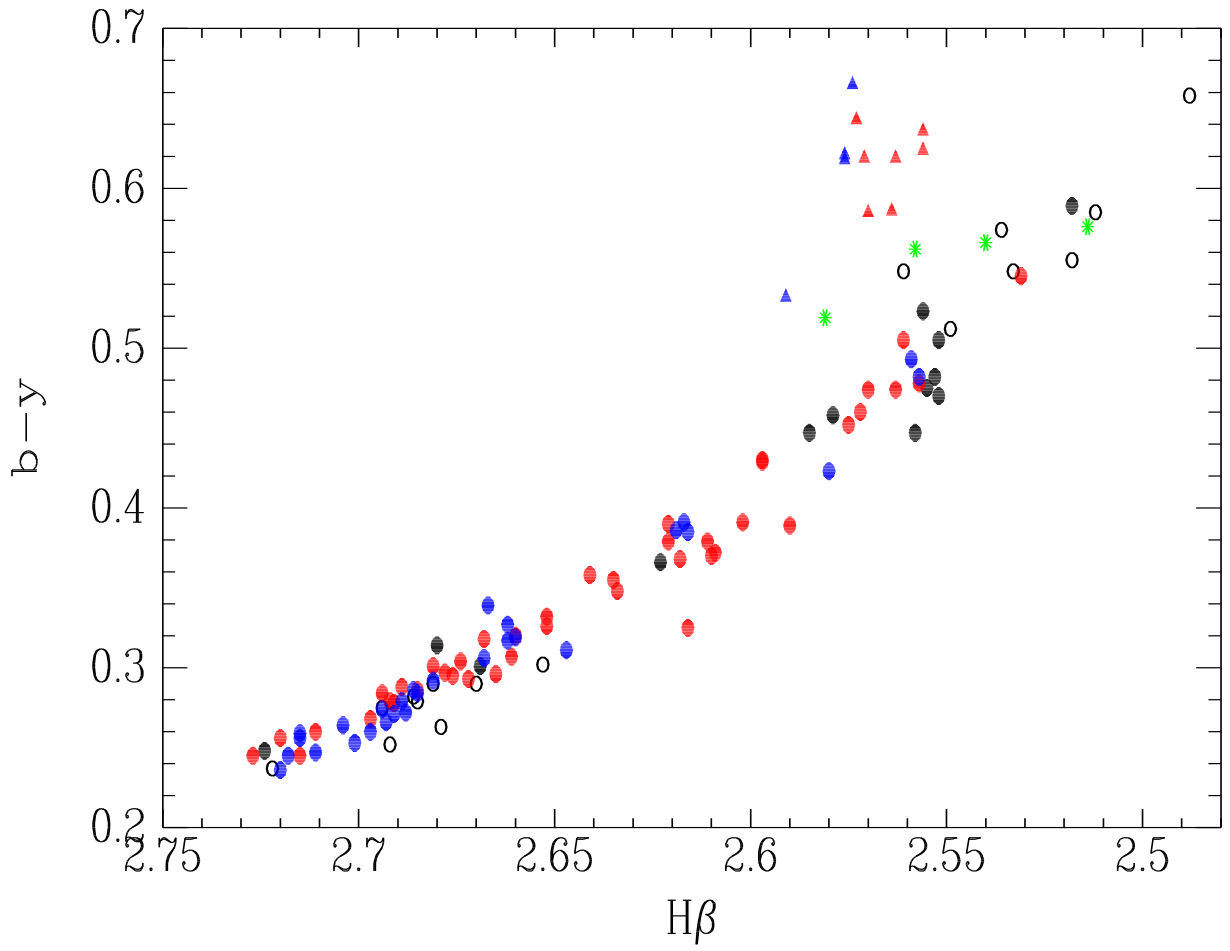


Fig. 8.— $(b - y)$, $H\beta$ relation for possible members of NGC 752. Symbols have the same meaning as Fig. 5.

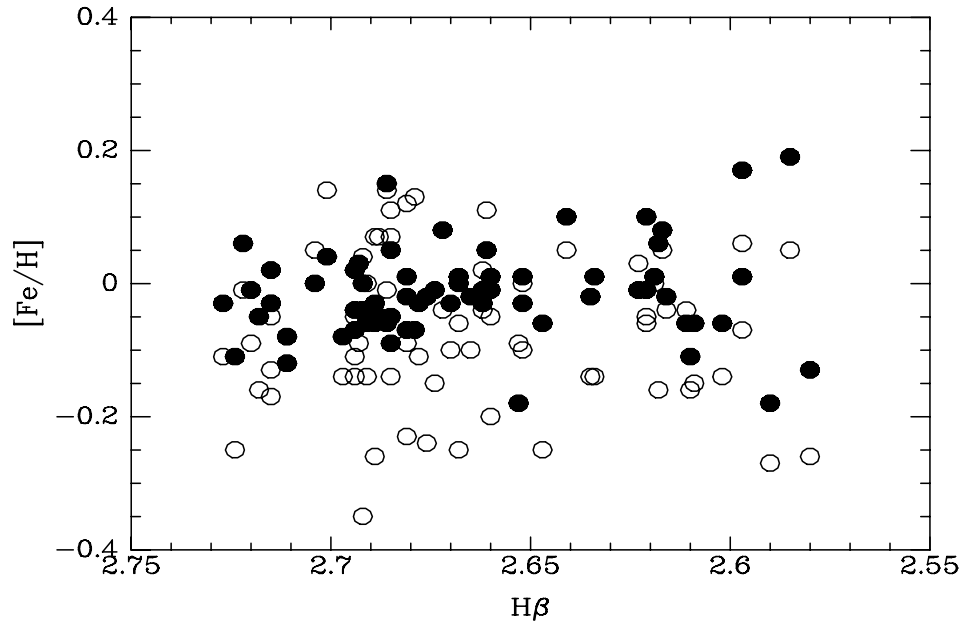


Fig. 9.— $[Fe/H]$ estimates from m_1 (open circles) and hk (filled circles) for 68 dwarfs as a function of $H\beta$.

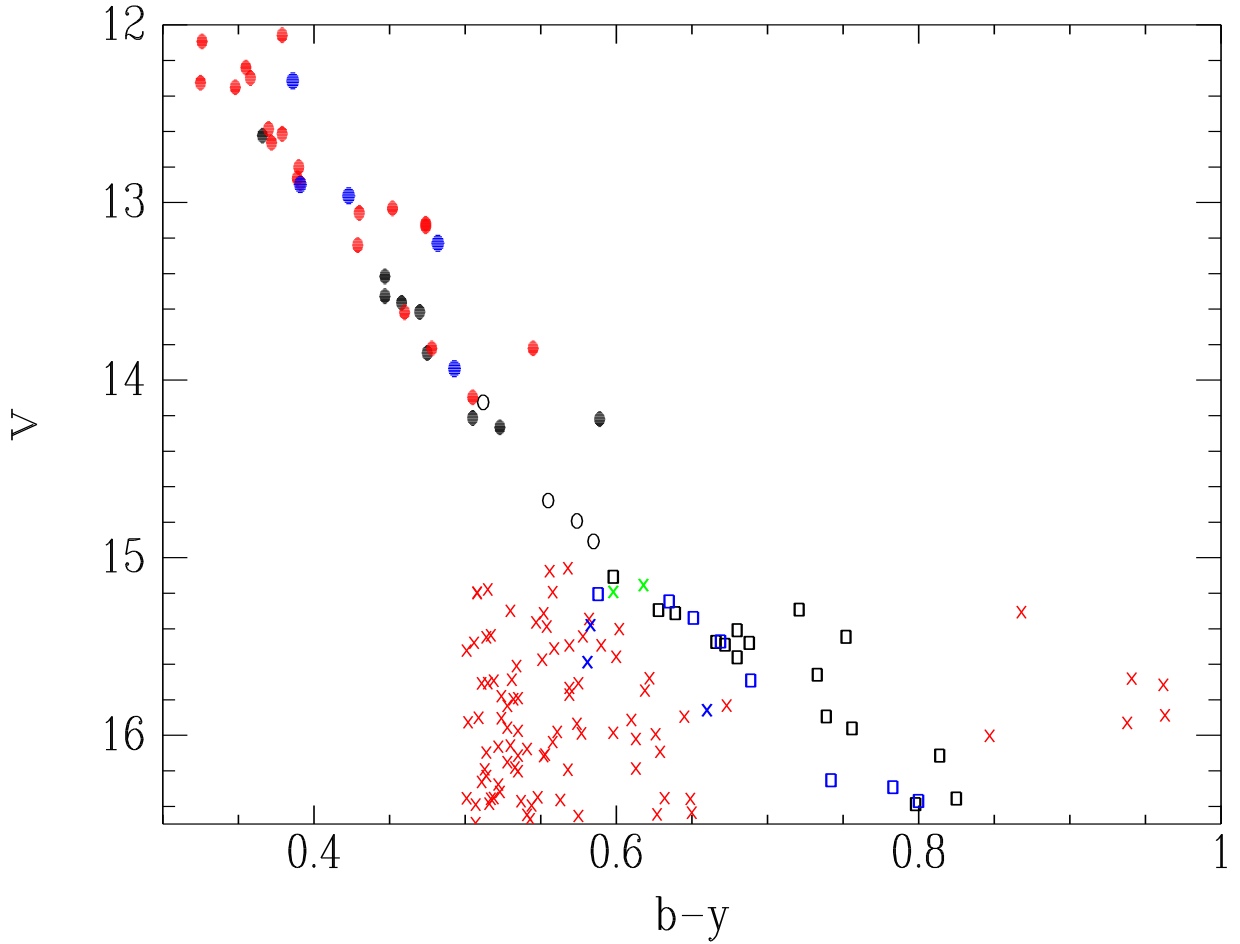


Fig. 10.— Identification of photometric members in the CMD. Symbols have the same meaning as in Fig. 5, with the addition of open black squares (16 probable members from our data alone), open blue squares (members in common with Bartašūište et al. (2011)), blue crosses (photometric members of Bartašūište et al. (2011) which we classify as nonmembers), red crosses (nonmembers from our data alone), and green crosses (stars with indices which classify them as evolved stars).

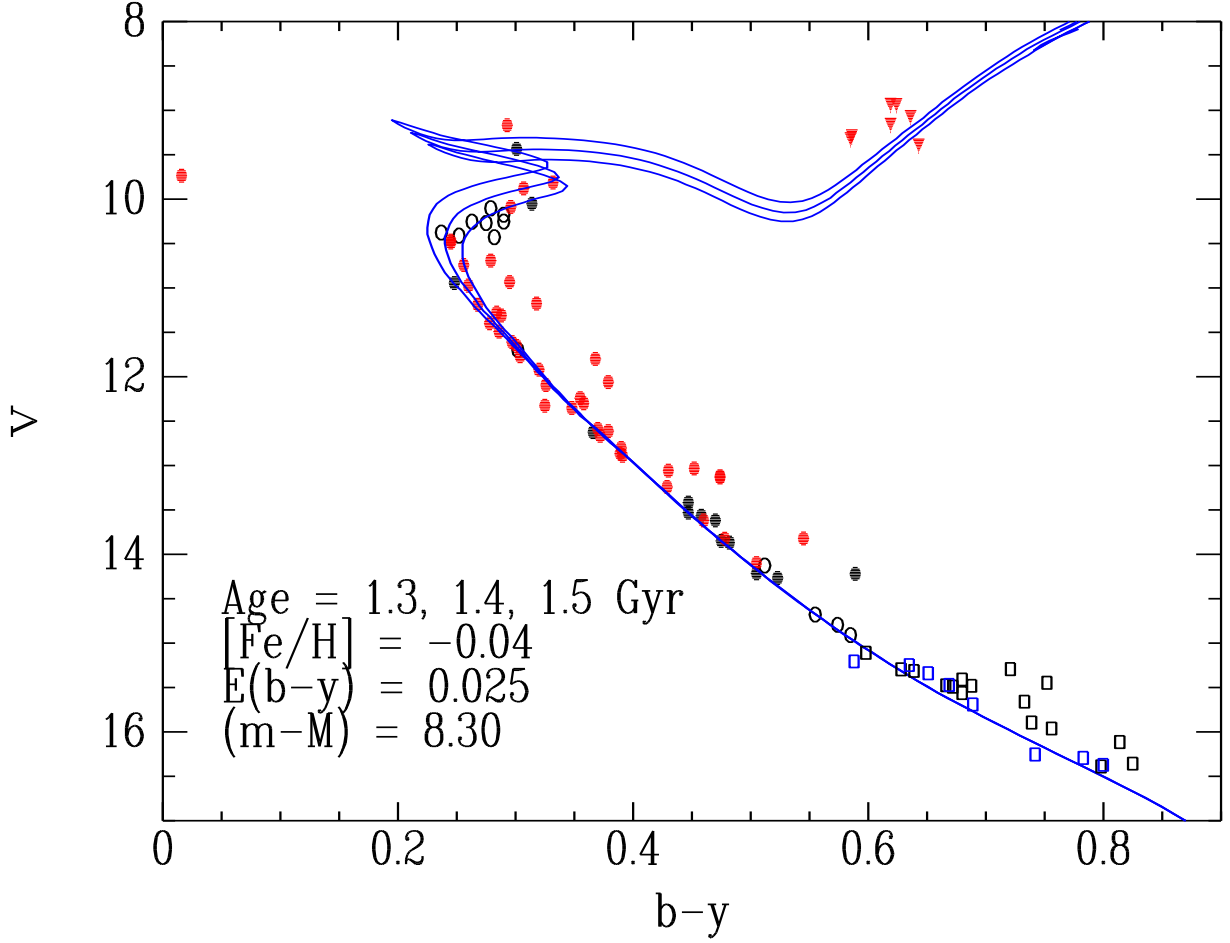


Fig. 11.— CMD fit of Victoria-Regina scaled solar isochrones to probable single-star members of NGC 752. Symbols have the same meaning as in Fig. 5 and Fig. 10. Isochrone ages are 1.3, 1.4, and 1.5 Gyr and have been adjusted to $E(b-y) = 0.025$ and $(m-M) = 8.30$.

Table 1. V magnitude Transformations

Source	N	Color Index	A	B	Std.Dev.	Excluded Stars
Johnson (1953)	37	$B - V$	-0.017	0.032	0.009	
Eggen (1963)	24	$B - V$	0.051	-0.048	0.020	
Jennens & Helfer (1975)	10		0.000	-0.026	0.012	
Twarog (1983)	17	$b - y$	-0.050	-0.002	0.008	
Rufener (1981, 1988)	39		0.000	-0.003	0.012	135, 201, 218, 273
Joner & Taylor (1995)	15		0.000	0.000	0.004	
Bartašūite et al. (2007)	37	$Y - V$	-0.048	0.022	0.007	88
Anthony-Twarog & Twarog (2007)	20		0.000	-0.024	0.008	

Note. — Coefficients A and B characterize the relationship between standard and source V magnitudes as follows: $V_{Standard} - V_{Source} = A(ColorIndex) + B$.

Table 2. Merged Photoelectric Secondary Standards in NGC 752

H number	V	sem	$b - y$	sem	m_1	sem	c_1	sem	H β	sem	hk	sem	Comments
27	9.148	0.004	0.627	0.009	0.368	0.013	0.408	0.015	0.000	0.000	1.091	0.012	
39	8.086	0.006	0.600	0.010	0.333	0.010	0.431	0.007	0.000	0.000	0.000	0.000	
58	10.489	0.007	0.260	0.001	0.149	0.008	0.621	0.011	2.707	0.008	0.445	0.033	Var?
61	10.043	0.003	0.249	0.005	0.155	0.008	0.669	0.011	2.708	0.008	0.000	0.000	
62	11.209	0.007	0.268	0.005	0.147	0.008	0.541	0.011	2.702	0.010	0.000	0.000	
64	10.537	0.004	0.239	0.001	0.168	0.008	0.686	0.011	2.734	0.008	0.430	0.023	
66	10.923	0.003	0.293	0.002	0.150	0.000	0.461	0.001	2.672	0.011	0.488	0.023	
75	8.966	0.003	0.622	0.026	0.362	0.039	0.420	0.020	0.000	0.000	1.079	0.033	
77	9.372	0.003	0.640	0.004	0.376	0.005	0.441	0.017	0.000	0.000	1.098	0.012	
88	11.759	0.002	0.324	0.001	0.149	0.005	0.426	0.007	2.654	0.010	0.000	0.000	
96	10.377	0.001	0.241	0.005	0.167	0.008	0.717	0.011	2.722	0.010	0.000	0.000	
105	10.257	0.003	0.274	0.002	0.153	0.008	0.667	0.011	2.692	0.008	0.453	0.001	
106	10.501	0.005	0.244	0.006	0.162	0.008	0.659	0.007	2.714	0.007	0.000	0.000	
108	9.161	0.002	0.295	0.003	0.160	0.004	0.635	0.004	2.679	0.004	0.000	0.000	
110	8.956	0.003	0.531	0.005	0.266	0.002	0.457	0.012	0.000	0.000	0.815	0.029	
126	10.101	0.003	0.284	0.001	0.140	0.008	0.640	0.011	2.684	0.008	0.474	0.013	
129	10.895	0.005	0.246	0.005	0.151	0.010	0.634	0.007	2.705	0.007	0.000	0.000	Var?
135	11.225	0.003	0.298	0.001	0.155	0.002	0.507	0.000	2.690	0.010	0.456	0.011	Con?
139	11.757	0.004	0.312	0.005	0.136	0.009	0.455	0.003	2.672	0.007	0.473	0.012	
166	9.857	0.001	0.261	0.003	0.158	0.005	0.644	0.004	2.700	0.004	0.000	0.000	
171	10.189	0.002	0.284	0.002	0.156	0.001	0.625	0.009	2.679	0.001	0.000	0.000	
177	10.170	0.004	0.317	0.002	0.152	0.004	0.566	0.004	0.000	0.000	0.000	0.000	
187	10.437	0.003	0.275	0.004	0.155	0.004	0.554	0.002	2.694	0.001	0.441	0.024	
189	11.284	0.003	0.280	0.002	0.145	0.000	0.516	0.001	2.692	0.008	0.447	0.033	
192	10.746	0.001	0.253	0.006	0.000	0.000	0.000	0.000	0.000	0.000	0.473	0.030	
193	10.202	0.002	0.239	0.002	0.192	0.001	0.714	0.002	2.726	0.004	0.445	0.009	
196	10.254	0.002	0.276	0.002	0.159	0.004	0.630	0.004	2.694	0.009	0.000	0.000	
197	11.602	0.002	0.294	0.003	0.154	0.005	0.467	0.005	2.678	0.008	0.000	0.000	
205	9.899	0.004	0.279	0.002	0.155	0.001	0.559	0.002	2.690	0.001	0.436	0.022	
206	10.019	0.004	0.313	0.001	0.153	0.003	0.581	0.005	2.671	0.002	0.436	0.013	
208	8.950	0.003	0.669	0.002	0.413	0.005	0.381	0.005	2.566	0.008	1.120	0.006	
209	9.741	0.002	0.018	0.002	0.166	0.001	0.991	0.002	2.919	0.001	0.286	0.016	
213	9.030	0.003	0.621	0.001	0.367	0.004	0.407	0.008	0.000	0.000	1.072	0.022	
217	10.428	0.001	0.282	0.002	0.152	0.006	0.636	0.003	2.696	0.001	0.000	0.000	
218	10.078	0.003	0.300	0.005	0.145	0.008	0.603	0.011	2.681	0.008	0.000	0.000	
220	9.593	0.002	0.604	0.004	0.405	0.006	0.370	0.008	2.575	0.005	0.000	0.000	
222	10.966	0.001	0.268	0.003	0.151	0.003	0.610	0.006	2.713	0.005	0.391	0.001	
234	10.679	0.003	0.279	0.003	0.156	0.006	0.570	0.002	2.706	0.007	0.455	0.026	
238	9.960	0.004	0.305	0.002	0.141	0.008	0.608	0.011	2.666	0.008	0.465	0.015	
254	10.920	0.005	0.242	0.005	0.156	0.007	0.652	0.010	2.713	0.006	0.414	0.014	
259	11.393	0.006	0.277	0.006	0.147	0.007	0.522	0.010	2.696	0.006	0.393	0.014	
261	11.174	0.002	0.315	0.001	0.160	0.004	0.434	0.003	2.671	0.008	0.000	0.000	
263	10.948	0.003	0.240	0.001	0.160	0.006	0.628	0.007	2.712	0.002	0.000	0.000	
266	11.229	0.009	0.277	0.005	0.152	0.007	0.526	0.010	2.702	0.008	0.000	0.000	
295	9.292	0.003	0.584	0.005	0.350	0.012	0.385	0.003	2.570	0.010	1.063	0.023	
300	9.595	0.003	0.258	0.006	0.146	0.004	0.647	0.005	2.692	0.005	0.478	0.020	
311	9.054	0.002	0.641	0.009	0.384	0.014	0.423	0.019	2.566	0.010	0.000	0.000	

Table 3. Calibration Coefficients

Index	Class	a	b	c	Num.	Residuals
V	all	1.000	0.041	1.581	105	0.010
hk	all	1.175	0.000	2.079	26	0.023
$H\beta$	blue	1.17	0.000	0.308	35	0.008
$H\beta$	red	1.12	0.000	0.411	38	0.008
$b - y$	evolved blue	1.067	0.000	0.243	46	0.005
$b - y$	red dwarf	0.900	0.000	0.276	14	0.005
m_1	blue	1.000	0.000	-0.954	35	0.008
m_1	evolved	1.000	-0.454	-0.839	24	0.014
m_1	red dwarf	1.000	0.450	-1.066	14	0.020
c_1	unevolved	1.095	0.000	0.189	49	0.025
c_1	evolved	1.000	0.338	0.148	25	0.031

Note. — For each index X_i , the calibrated value is $a_i X_i + b_i(b - y)_{instr} + c_i$.

Table 4. Photometry in NGC 752

$\alpha(2000)$	$\delta(2000)$	V	$b-y$	m_1	c_1	hk	$H\beta$	σ_V	σ_{by}	σ_{m1}	σ_{c1}	σ_{hk}	σ_β	N_y	N_b	N_v	N_u	N_{Ca}	N_n	N_w	WEBDA	ID_{PL}	ID_H	ID_{RV}	ID_{ST}	Memb.	Class
1.961863	37.66953	7.119	0.741	0.535	0.394	1.335	9.999	0.003	0.008	0.013	0.012	0.012	9.999	7	7	17	18	34	0	0	215	882	215	1	285	0	G
1.932012	37.86701	8.085	0.596	0.342	0.417	1.049	2.572	0.003	0.006	0.008	0.006	0.008	0.006	17	15	15	17	23	7	6	39	394	39	26	64	0	G
1.980912	37.68589	8.357	0.082	0.203	0.985	0.370	2.871	0.006	0.008	0.016	0.020	0.012	0.011	5	5	5	7	6	1	1	309	1168	309	64	394	0	B
1.927771	37.88174	8.917	0.619	0.361	0.438	1.099	2.563	0.002	0.003	0.004	0.003	0.004	0.003	7	7	6	7	8	2	2	24	350	24	25	41	99	G
1.950852	38.13387	8.920	0.624	0.378	0.395	1.104	2.556	0.002	0.003	0.004	0.004	0.003	0.002	14	12	15	17	17	6	5	137	687	137	0	202	99	G
1.960438	37.66030	8.940	0.665	0.397	0.390	1.147	2.574	0.001	0.002	0.003	0.003	0.003	0.003	30	29	20	20	35	18	16	208	858	208	0	278	99	G
1.947371	38.03264	8.953	0.532	0.273	0.435	0.797	2.591	0.002	0.003	0.004	0.004	0.004	0.002	19	18	19	21	23	9	9	110	630	110	33	174	95	G
1.938685	37.96680	8.967	0.618	0.362	0.432	1.100	2.576	0.002	0.003	0.006	0.007	0.004	0.008	11	12	12	12	15	6	6	75	506	75	29	119	98	G
1.960795	37.76987	9.023	0.621	0.369	0.400	1.074	2.576	0.002	0.002	0.003	0.003	0.003	0.002	40	38	34	36	49	21	19	213	867	213	60	283	99	G
1.981216	37.81636	9.054	0.636	0.398	0.385	1.116	2.556	0.001	0.002	0.004	0.004	0.004	0.003	15	16	16	18	18	7	5	311	1172	311	65	397	99	G
1.928551	37.63222	9.143	0.619	0.374	0.416	1.083	2.571	0.004	0.004	0.006	0.006	0.005	0.005	8	8	6	7	9	4	3	27	356	27	20	47	99	G
1.971785	37.80309	9.149	0.213	0.154	0.630	0.413	2.733	0.003	0.005	0.008	0.008	0.007	0.004	31	26	21	25	30	20	15	271	1033	271	62	349	0	B
1.947187	38.02248	9.167	0.293	0.150	0.660	0.504	2.672	0.001	0.003	0.004	0.005	0.004	0.004	20	20	18	21	22	9	8	108	626	108	32	169	99	B
1.924571	37.99932	9.273	0.586	0.333	0.436	1.030	2.564	0.002	0.004	0.006	0.006	0.006	0.006	9	8	6	6	9	4	4	11	308	11	0	21	94	G
1.974815	37.86064	9.305	0.585	0.354	0.382	1.030	2.570	0.003	0.004	0.004	0.004	0.005	0.005	24	26	22	23	30	17	15	295	1089	295	67	377	99	G
1.939415	37.60233	9.376	0.643	0.375	0.441	1.116	2.573	0.003	0.004	0.005	0.004	0.004	0.004	13	14	12	12	15	8	7	77	512	77	45	123	98	G
1.953353	37.98999	9.434	0.301	0.170	0.594	0.563	2.669	0.002	0.002	0.004	0.004	0.004	0.004	24	22	24	26	30	16	13	159	728	159	0	225	99	B
1.962645	37.65648	9.571	0.607	0.391	0.406	1.069	2.578	0.002	0.003	0.004	0.005	0.005	0.004	34	34	20	20	35	21	20	220	895	220	0	290	0	G
1.976816	37.75319	9.595	0.272	0.159	0.608	0.446	2.688	0.003	0.004	0.005	0.005	0.005	0.003	23	22	21	22	24	11	10	300	1117	300	63	382	99	B
1.932206	38.04229	9.698	0.995	0.769	0.120	2.030	2.574	0.002	0.003	0.007	0.010	0.005	0.002	15	15	12	12	15	8	8	40	398	40	474	65	0	G

Note. — In addition to identifications from the WEBDA database, identifications from Platais (1991), Heinemann (1926), Rohlf & Vanysek (1961) and Stock (1985) are included. The final columns denote the membership probability from Platais (1991) and the calibration equation class.